AD-A040 469 STANFORD RESEARCH INST MENLO PARK CALIF F/G 9/5
ELECTRONICALLY TUNABLE UHF HIGH-POWER FILTER.(U)
MAY 77 A KARP F30602-76-C-0248
UNCLASSIFIED RADC-TR-77-167 NL

1 OF 1
AD A040469

END
DATE FILMED
7-77

AD A040469

12
NW

RADC-TR-77-167
Final Technical Report
May 1977

ELECTRONICALLY TUNABLE UHF HIGH-POWER FILTER

Stanford Research Institute

Approved for public release; distribution unlimited.

AD No.
DDC FILE COPY

ROME AIR DEVELOPMENT CENTER
Air Force Systems Command
Griffiss Air Force Base, New York 13441

DDC
RECEIVED
JUN 13 1977
B

This report has been reviewed by the RADC Information Office (OI) and is releasable to the National Technical Information Service (NTIS). At NTIS it will be releasable to the general public, including foreign nations.

This report has been reviewed and is approved for publication.

APPROVED: Thomas E. Baustert

THOMAS E. BAUSTERT
Project Engineer

APPROVED: Joseph J. Naresky

JOSEPH J. NARESKY
Chief, Reliability & Compatibility Division

FOR THE COMMANDER: John P. Huss

JOHN P. HUSS
Acting Chief, Plans Office

Do not return this copy. Retain or destroy.

UNCLASSIFIED

SECURITY CLASSIFICATION OF THIS PAGE (When Data Entered)

REPORT DOCUMENTATION PAGE

READ INSTRUCTIONS BEFORE COMPLETING FORM

1. REPORT NUMBER: RADC-TR-77-167	2. GOVT ACCESSION NO.
3. RECIPIENT'S CATALOG NUMBER	
4. TITLE (and Subtitle): ELECTRONICALLY TUNABLE UHF HIGH-POWER FILTER	5. TYPE OF REPORT & PERIOD COVERED: Final Technical Report. 4 May 76 — 3 Feb 77
6. PERFORMING ORG. REPORT NUMBER: SRI Project 5370	
7. AUTHOR(s): Arthur Karp	8. CONTRACT OR GRANT NUMBER(s): F30602-76-C-0248
9. PERFORMING ORGANIZATION NAME AND ADDRESS: Stanford Research Institute, Menlo Park CA 94025	10. PROGRAM ELEMENT, PROJECT, TASK AREA & WORK UNIT NUMBERS: 62702F, 45400355
11. CONTROLLING OFFICE NAME AND ADDRESS: Rome Air Development Center (RBCT), Griffiss AFB NY 13441	12. REPORT DATE: May 1977
	13. NUMBER OF PAGES: 71 (12) 75p.
14. MONITORING AGENCY NAME & ADDRESS (if different from Controlling Office): Same	15. SECURITY CLASS. (of this report): UNCLASSIFIED
	15a. DECLASSIFICATION/DOWNGRADING SCHEDULE: N/A

16. DISTRIBUTION STATEMENT (of this Report)

Approved for public release; distribution unlimited.

17. DISTRIBUTION STATEMENT (of the abstract entered in Block 20, if different from Report)

Same

18. SUPPLEMENTARY NOTES

RADC Project Engineer:
Thomas E. Baustert (RBCT)

19. KEY WORDS (Continue on reverse side if necessary and identify by block number)

Electronically tunable resonator	High-power resonator
Electronically tunable filter	Electromagnetic Compatibility
ETF	UHF resonator
Electronic tuning	UHF filter
PIN-diode switching	Bandpass filter

(See reverse)

20. ABSTRACT (Continue on reverse side if necessary and identify by block number)

This report describes a research and development program that established the feasibility of a low-loss, high-power UHF resonator with electronic tuning means based on the "L-Flauto" principle. This principle provides for changing the resonant frequency of a transmission-line cavity in discrete steps by using arrays of PIN diodes to short out inductances that are in series with the line. In an appropriate design, N switched inductances would provide 2^N tuning channels selectable under binary-logic control. This kind of resonator has application to interference reduction in frequency-agile Air Force communication systems,

DD FORM 1 JAN 73 1473 EDITION OF 1 NOV 65 IS OBSOLETE

UNCLASSIFIED

SECURITY CLASSIFICATION OF THIS PAGE (When Data Entered)

332500

Block 19. (continued)

Interference reduction
Air Force communications systems

Block 20. (continued)

where it would be used as a fast-tuning bandpass filter or as a tank circuit for a transmitter output stage.

To demonstrate feasibility, a simple experimental resonator including only two tuning inductances was developed. One inductance corresponds to Tuning Inductance 1; the other is of equal value and functions as a surrogate for Tuning Inductances 2, 3, 4, . . ., N. Each inductance was realized as a radial line stub extending from the outer conductor of the coaxial-line cavity. The entrance to the radial line is spanned by an array of six paralleled Unitrode UM 4010 C diode pairs, with bias applied to the common-anode point for each back-to-back pair.

The feasibility-model resonator thus has a tuning channel at each end of an overall tuning range of 349 to 391 MHz, and also a degenerate pair of tuning channels at 368 MHz. The resonator has an unloaded Q ranging between 1700 and 2560, so that for a loaded bandwidth of about 0.9%, the insertion loss is 0.5 to 0.6 dB. For this loaded bandwidth, the RF input power rating is in excess of 1000 W on a CW basis, indicating that the resonator can continuously withstand in excess of 140 kVA internally.

The R&D program included modeling the resonator and the tuning means, developing design relationships, and selecting a PIN-diode type and a corresponding grouping scheme. Also included were the development of a mechanical design permitting performance evaluation in a simple and economical way, and the experimental validation of the design principles through testing at low RF input power levels and at high power levels up to 1250 W, CW.

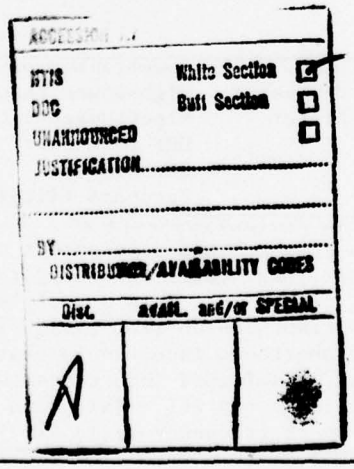

CONTENTS

LIST OF ILLUSTRATIONS v

LIST OF TABLES vi

ACKNOWLEDGMENTS vii

I INTRODUCTION AND BACKGROUND 1

II SCOPE AND OBJECTIVES 7

III MODELING AND DESIGN RELATIONS 11

A. General 11

B. Basic Resonator 12

C. Radial-Line-Stub Inductances 14

D. Relation of Tuning Range to Stub Reactance 15

E. RF Voltages and Currents in the Resonator 15

F. Switch Stresses and Dissipation 17

1. Forward-Bias Case 18
2. Reverse-Bias Case 19

G. Calculation of Unloaded Q 20

1. Forward-Bias Case 21
2. Reverse-Bias Case 21

H. Optimum Number of Diode Pairs in Parallel 22

I. Summary of Design Parameters 24

IV FEASIBILITY MODEL DESIGN AND CONSTRUCTION 27

A. General 27

B. Diode Selection 29

C. Resonator Details 30

D. Bias Means 32

E. Coupling Probes 34

V LOW-POWER TEST RESULTS 37

A. Weak External Coupling 37

1. Dummy Diodes Installed 37
2. Actual Diodes Installed 39

B. Strong External Coupling 41

VI HIGH-POWER TEST RESULTS 43

VII CONCLUSIONS 49

VIII OPTIONS FOR FUTURE WORK 53

A. Extension of Current Work 53

B. Alternative Approach 56

C. Other Areas of Application 57

APPENDICES

A EFFECTS OF FINITE DIODE REACTANCE ON DESIGN RELATIONS 59

B DERIVATION OF EXPRESSIONS FOR UNLOADED Q 65

REFERENCES 71

ILLUSTRATIONS

1	"C-Flauto" Resonator Tuning Scheme	3
2	"L-Flauto" Resonator Tuning Scheme	5
3	Resonator of Figure 2 Simplified for Feasibility Demonstration Purposes	9
4	Basic Configuration of Feasibility-Model Filter Resonator	13
5	Use of Back-to-Back PIN-Diode Pair as Switch Across Inductive Stub	17
6	Equivalent Circuit of Tuning Element with Diode Parasitics Included	18
7	Dependence of Overall Q_u on Cavity Q_u for Z_0 = 63 ohms and Tuning Elements Having n Pairs of Forward-Biased Diodes for which R_s = 0.05 ohm	22
8	Dependence of Overall Q_u on Cavity Q_u for Z_0 = 63 ohms and Tuning Elements Giving f_{0A}/f_{0B} = 0.89 and Having n Pairs of Reverse-Biased Diodes for which R_p = 70,000 ohms	23
9	Developmental Feasibility Model of High-Power UHF Bandpass Filter with L-Type Electronic Tuning	28
10	Essential Configuration of Developmental Electronically Tuned UHF Filter Resonator	31
11	Constructional Details in Vicinity of a Diode Pair	33
12	Unitrode UM 4010 C PIN Diode and Brass "Dummy" Screwed into a Heat-Sink Plate	38
13	Variation of Overall Q_u with Bias Current at f_{0B} = 401.6 MHz	40
14	Block Diagram of High-Power CW UHF Test Facility	44
15	Schematic Representation of UHF Bandpass Filter and Diode Biasing Means	46
16	Insertion Loss vs Reverse-Bias Voltage for High-Power Operation at f_{0A}	47
17	Variation of Insertion Loss with Forward-Bias Current at f_{0B}	48
18	Possible Configurations for Multichannel L-Type High-Power UHF Filter Resonators, Drawn to a Scale of About 1:3.3	55

19 Alternative Configuration for Multichannel L-Type UHF Filter Resonator with Same Performance as that of Figure 18(a), Drawn to Same Scale 56

B-1 Equivalent Circuit, Using Slope-Parameter Values, for Resonator with Forward-Biased Diodes at Frequency f_{OB} 68

B-2 Equivalent Circuit, Using Slope-Parameter Values, for Resonator with Reverse-Biased Diodes at Frequency f_{OA} 68

TABLE

1 Performance Data of Feasibility Model Bandpass Filter 42

ACKNOWLEDGMENTS

The suggestions and contributions made by the following SRI staff members, in the areas indicated, are hereby acknowledged:

Louis N. Heynick	**Project Supervision**
Ulrich H. Gysel	**Filter and resonator relationships**
John P. Watjen	**High-power test setups and procedures**
Leroy M. Lumbard	**Mechanical design and fabrication**
R.R. Evans, J.H. Hunt, H.J. Jacobs, and other Radio Physics Laboratory Engineering Assistants (supervised by L. Coomer)	**Miscellaneous technical assistance**

The encouragement and guidance of William A. Edson contributed importantly to the project. Don Parker (now departed from SRI), along with Mr. Heynick and Dr. Edson, provided valuable support while concepts were being formulated and sponsorship was being sought for the new direction of research undertaken here.

As the mediator of the Air Force Systems Command's sponsorship, RADC monitor Mr. Thomas E. Baustert was an expert and tireless facilitator, thereby greatly aiding the successful completion of the contract.

The cooperation of Mr. Gerald Hiller, Unitrode Corporation, Watertown, Massachusetts, is hereby once again acknowledged in the matter of PIN-diode application.

EVALUATION

The feasibility of a low-loss, high power UHF resonator with electronic tuning means was established on this effort. All of the original design objectives were met by Stanford Research Institute. The technology developed on this effort can be used to design high power filters for use on frequency-agile communication systems and radars. This design uses the "L-Flauto" principal where the resonant frequency of a transmission line cavity can be changed in discrete steps by using arrays of PIN diodes to short out inductances which are effectively in series with the line. No effort was made to reduce the volume of the filter because the intent was only to demonstrate electrical feasibility. The modeling has shown that all the transverse dimensions can be halved with only a small effect on the filter performance. The agreement between predicted and observed performance data attests to the aptness and validity of the equivalent-circuit modeling and of the design relations developed. Future design work can thus be undertaken with confidence in the predicted outcome.

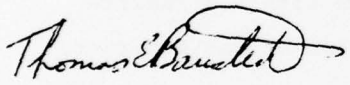

THOMAS E. BAUSTERT
Project Engineer

I INTRODUCTION AND BACKGROUND

Air Force UHF communications systems for ground/air/satellite applications have a serious present and future need for electronically tunable bandpass filters (ETFs) with a high RF power rating along with the necessary high selectivity and low insertion loss. When connected to a transmitter of the "frequency-agile" type, such a filter prevents spurious wideband energy from reaching the antenna and also provides isolation for collocated transmitters and receivers. The term "frequency agility" or "frequency hopping" denotes transmission and reception over a number of continuously changing frequency channels. The allowable switching time in such systems is so brief (< 50 μs) that existing mechanically tuned filters are unsatisfactory.

The RF power rating of bandpass filters for such systems is a paramount consideration. The power levels of interest range from 100 W to 1000 W, CW, and beyond. The familiar varactor and YIG tuning techniques, which are associated with RF power levels of the order of milliwatts, are clearly unsuitable.

This report summarizes a nine-month exploratory developmental program that has established the feasibility of a heretofore untested concept for electronically tuning the high-Q resonator of a UHF bandpass filter in finite frequency steps. The concept, denoted "L-Flauto," is based on incrementally switching series inductance by means of PIN diodes. A minimum CW power rating of 1000 W was made a principal design objective to comply with the trend in Air Force communications systems and to demonstrate the future usefulness of the concept.

A low-loss resonator with a high power rating and "fast" (i.e., electronic) tuning need not be limited in application to bandpass filters; the resonator could provide a fast-tuned "tank" circuit for a transmitter amplifier stage.

Prior to initiating the present program, two contracts had been completed for RADC.[1,2*] Under those programs, the feasibility and usefulness of the electronic resonator-tuning scheme now referred to as "C-type" was amply demonstrated. All this work was based on loading a coaxial-line resonator with a set of two-valued shunt capacitances (see Figure 1). These capacitances are essentially equal, but--very importantly--they are spatially distributed. Moreover, this capacitive loading is characterized as relatively "light," because the necessary foreshortening of the half-wave resonator amounted to only about 13% to 23%. This kind of design proved fairly easy to work with, for the distances between adjacent tuning reactances within the resonator were electrically and mechanically ample. The value of transmission-line Z_0 chosen (56 ohms) was within the range (35 to 75 ohms) that is mechanically convenient. PIN diode selection was guided by the need for a high voltage rating to yield a high filter power rating, and by the need for the least diode capacitance available at this voltage rating to maintain the condition of light capacitive loading.

The goals of the two prior contracts were ultimately achieved in an operating second-order bandpass filter.[†] These goals included optimization of the uniformity of spacing of the numerous (128) tuning channels made available within a 45-MHz tuning range (355 to 400 MHz) by the small number (seven) of independent tuning capacitances. They also entailed the achievement of close tracking of all the tuning channels of one resonator against those of a duplicate resonator so that a second-order electronically tunable filter could be realized. The peak RF power rating of this filter was limited to about 100 W by the diode voltage stress, as determined by the percentage tuning range and the resonator Z_0, electrical length, and loaded Q. The CW power rating had the same value, since the thermal stress on the diodes is relatively low, even in the

---

*References are listed at the end of the report.

†See Section I-B of Ref. 2.

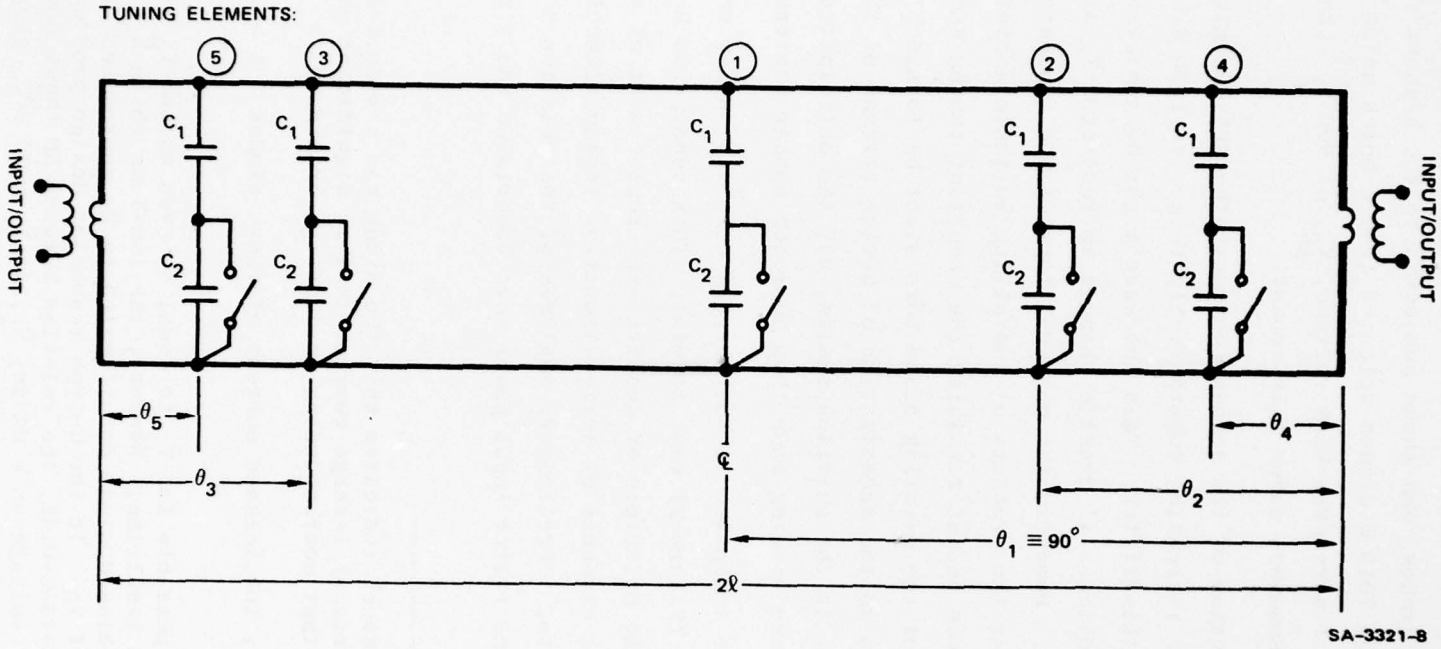

FIGURE 1 "C-FLAUTO" RESONATOR TUNING SCHEME. Transmission-line segment lightly and distributively loaded with two-valued shunt capacitances, providing a binary-scaled series of tuning increments.

worst case. The PIN diodes in this design are "soft-knee"* Unitrode series UM 7000 C diodes, and those subjected to the highest voltage stress are type UM 7010 C diodes selected from a batch so as to permit the application of a reverse-bias voltage, V_0, of 900 V,† and a peak RF voltage, $\hat{V}_1$, of somewhat under this amount.‡

After completion of the second contract, thought was given to the possibilities for increasing substantially (e.g., to 1000 W) the RF power rating of this filter. This increase might be achievable with the same diode voltages if drastic changes in resonator Z_0 or electrical length were made. However, the physical form of the resonator would then be so altered that the problems of installing suitable noninteracting tuning capacitances and of retaining the excellent tuning and tracking characteristics of the existing resonators might be formidable. Serious thought was given to the substitution of series strings of three PIN diodes (or chips) in the existing design, but the anticipated complexities of heat sinking and biasing made this approach appear unattractive.

Prior to the inception of the current contract, a new concept in resonator tuning (Figure 2) came to mind. This concept is based on an application of the principle of duality--the replacement of shunt-capacitive tuning elements by series-inductive tuning elements, whence the term "L-Flauto." Preliminary analyses of the relation between switch voltage and filter input power were undertaken and yielded

---

*The term "soft-knee" indicates that the diode has a wide I-layer and therefore a (surface) leakage current that is significant at reverse voltages below that corresponding to junction breakdown.

†At this voltage, the leakage current of these diodes ≤ 1 μA at room temperature.

‡It is actually possible for $\hat{V}_1$ to equal or even exceed V_0 without forward conduction resulting. However, the low-loss (high R_p) character of the reverse-biased diode deteriorates as $\hat{V}_1$ approaches within roughly 100 V of V_0. In the C-type resonator design produced under Contract F30602-74-C-0142, the relation between RF input power, P_0, and the peak RF voltage on a diode, $\hat{V}_1$, is $\hat{V}_1 \approx 75\sqrt{P_0}$, RADC-TR-75-220, (A018044).

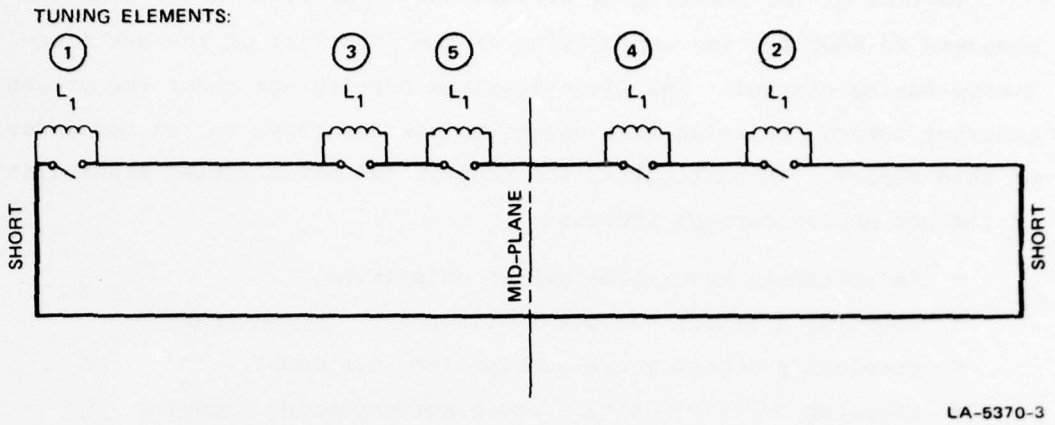

FIGURE 2 "L-FLAUTO" RESONATOR TUNING SCHEME. Transmission-line segment distributively loaded with switchable series inductances, providing a series of binary-scaled tuning increments. Switch parasitics and external coupling to resonator not shown.

encouraging results. In particular, it was predicted that a power rating of 1000 W could be obtained through L-type tuning of the coaxial resonator and with diode voltage stresses about the same as previously. In these calculations, the constraints imposed, which are the same as those for the previous contract,[2] were the following:

- An overall tuning range of roughly 12%.
- External two-port loading sufficient to make the loaded bandwidth about 0.9%.*
- "Light" reactive loading of the coaxial-line resonator--that is, installation of the tuning reactances would necessitate only a modest foreshortening of the resonator.
- Convenient values of resonator Z_0; that is, $35 < Z_0 < 75$ ohms.

---

*This is equivalent to specifying a loaded Q, Q_L, of about 110, or else an external Q, Q_E, of about 250, since $(1/Q_L) = (2/Q_E) + (1/Q_u)$, where the unloaded Q, Q_u, is typically 1000. The RF power rating of a filter is significant only in relation to the loaded fractional bandwidth because the reactive voltamperes circulating within the resonator are some $(4/\pi)$ Q_L times greater than the filter input power. Thus, the specifications given imply that the resonator must withstand about 140 kVA internally.

In view of the encouraging predictions, a development program was proposed to RADC for the exploration of the potential of the new electronic-tuning concept. The investigations carried out under the present contract toward achieving this objective are described in the remainder of this report. In particular, the program for establishing feasibility of the new design concept included:

- Establishing meaningful design objectives.
- Modeling a filter resonator with L-type tuning means.
- Developing design relationships for this model.
- Choosing a PIN diode type and a corresponding grouping scheme.
- Developing the mechanical design of a filter that would permit performance evaluation, yet be simple and economical.
- Predicting the performance of this design.
- Constructing an experimental filter of this design and testing it under "small-signal" conditions and then under 1000 W of RF input power, CW, and perhaps higher.

II SCOPE AND OBJECTIVES

The overall objective of this contract was to establish the feasibility of a UHF bandpass filter having an RF input power rating of 1000 W, CW, and electronic tuning means based on the L-Flauto principle. This principle, in essence, consists of altering the resonant frequency of a length of coaxial (or other) transmission line by using PIN-diode switches to short out inductances that are in series with the line. As illustrated in Figure 2, the resonator of a fully operational bandpass filter employing this principle might have several identical inductive reactances and their associated switches. If the coaxial-line resonator has a short at both ends (the simplest of several possible arrangements), the tuning element located closest to either short provides the largest tuning increment, which is one-half of the total tuning range, when the state of its switch is changed. This switch would be controlled by the most-significant bit of a binary-coded tuning command logic.

The second bit of the tuning command logic would control the switch associated with Tuning Element 2, which would provide a tuning increment of one-fourth of the total tuning range. Since the inductance is nominally the same in every tuning element, the reduction in tuning increment would be obtained by locating Tuning Element 2 away from a short and toward the resonator mid-plane, where the RF currents are weaker. Since the switches in each tuning element are assumed to have the same properties, it can be shown that any RF power dissipated in Tuning Element 2 should be half that dissipated in Tuning Element 1. This is consistent with the fact that any RF current or voltage associated with Tuning Element 2 should be $\sqrt{1/2}$ times that associated with Tuning Element 1.

Similarly, Tuning Elements 3, 4, 5, . . ., N would have the same form as 1 and 2, but be located progressively closer to the resonator mid-plane. Thus, a series of tuning increments (expressed as fractions

of the total tuning range) equal to

$$\frac{1}{2}, \frac{1}{4}, \frac{1}{8}, \ldots, 1/2^N$$

would be provided by Tuning Elements 1, 2, 3, . . ., N. Additionally, the RF power dissipation associated with each tuning element (expressed as fractions of the total power dissipated in the tuning elements) can also be given by the same series.

The construction and testing of an L-type electronically tunable filter having all the features of Figure 2 would be relatively costly without benefit of previous developmental work. Hence, a simplified feasibility model was proposed and investigated. This model made use of the fact that

$$\frac{1}{4} + \frac{1}{8} + \frac{1}{16} + \ldots + 2^{-N} \approx \frac{1}{2}$$

when N is large. That is, in the series expressing both relative tuning increment and relative RF power dissipation, the sum of the second through Nth terms is very nearly equal to the first term. It was thus possible to develop a feasibility-model filter resonator loaded only with Tuning Element 1 and a duplicate thereof to act as a surrogate for all the less significant tuning elements, as shown in Figure 3. The important parameters (total tuning range, power rating, Q_u, Q_L, and Q_E) of this model, whose symmetry greatly facilitates modeling and analysis, are the same as those of the multichannel filter of Figure 2 because everything that determines these parameters is accounted for. The only important difference is that the simplified filter model has three, instead of 2^N, tuning channels--one at the lower extremity of the tuning range (both switches open), another at the upper extremity (both switches closed), and the third at an intermediate frequency (one switch open and

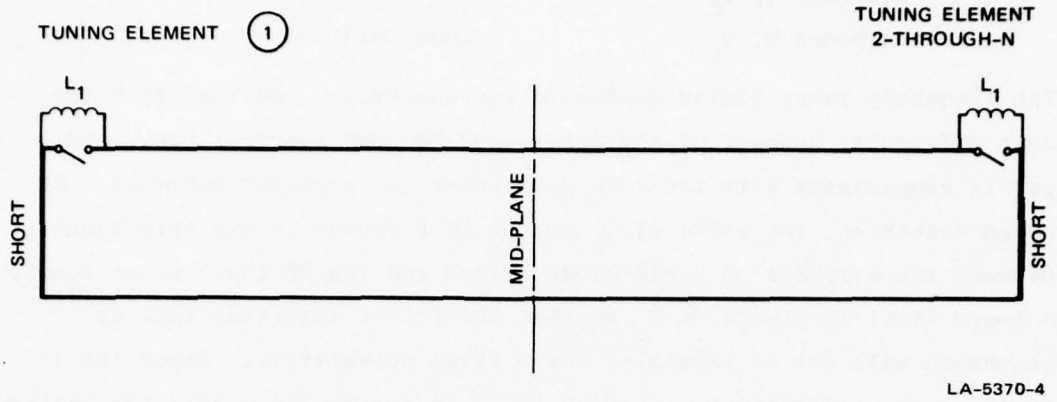

FIGURE 3 RESONATOR OF FIGURE 2 SIMPLIFIED FOR FEASIBILITY DEMONSTRATION PURPOSES. Tuning element at right end is surrogate for Tuning Elements 2, 3, 4, ..., N. Switch parasitics and external coupling to resonator not shown.

the other closed).* For this configuration, the simplest and most convenient devices for obtaining input and output coupling are a pair of adjustable capacitive probes inserted near the resonator mid-plane. The external Q, Q_E, and hence the loaded Q, Q_L, could be set by adjusting (equally) the penetration of these coupling probes. The coaxial lines and connectors associated with the probes establish an input and output reference impedance level of 50 ohms.

In summary, the scope of this contract was confined to analyzing, designing, constructing, and testing the high-Q_u, high-power bandpass filter illustrated schematically in Figure 3.

The basic design objectives for the developmental single-resonator filter were:

Frequency range limits	355 and 400 MHz
RF input power rating	1000 W, CW

*This simplification avoids the necessity of developing "trimming" means for the tuning-element reactance. In a future development, fine adjustment of each tuning-element reactance (see Figure 2) would be necessary to complete a fully operational filter, especially if it is a multiresonator filter. (See Sections IV-B-2 and V-I of Ref. 2.)

External Q, Q_E	250
Unloaded Q, Q_u	1000, minimum

The frequency range limits demarcate the uppermost, and therefore the most difficult, quarter of the 225-to-400-MHz UHF spectral band, and permit comparisons with the work done under the previous contract. As noted elsewhere, the value of Q_E chosen is a factor in the relationship between the stresses on a PIN-diode switch and the RF input power level. A lower limit is placed on Q_u so that the filter insertion loss at resonance will not be excessive for a given selectivity. Since the insertion loss indicates how much RF power is dissipated within the filter, its value also dictates what means may be necessary for evacuating the heat developed in a tuning element so that excessive diode temperatures will not occur when the rated RF power is applied continuously.

Since the current work was exploratory in nature, no design objectives were established regarding the practical concerns of size, weight, and environmental effects. However, it was recognized that the future usefulness of the techniques explored will depend in part on what might eventually be accomplished with regard to these concerns. Furthermore, no design objectives were specified regarding tuning speed, which relates to the design of the PIN-diode driving circuitry eventually needed. However, the filter performance was not made dependent on any components that might be incompatible with the diode drivers that are ultimately adopted.

III MODELING AND DESIGN RELATIONS

A. General

This section concerns the parameters of the symmetrically tuned filter resonator, and their relationships to one another. The parameters that depend on the mechanical dimensions of the resonator are considered first, after which the relationship between tuning range and tuning reactance is established. The large RF currents and voltages that build up within the resonator, due to the large value of Q_L (or Q_E), are expressed relative to the RF input power. Subsequently, the groupings of PIN diodes that constitute the switches are described and the thermal and voltage stresses per diode are established, along with the total diode dissipations for each tuning element. These latter quantities are used in determining overall resonator Q_u values, which are important because good design requires Q_u to be as large as is practical over the entire tuning range. (To best achieve this, it follows that Q_u should be as uniform as is practicable over the tuning range.)

To keep this section concise, derivations are omitted when it is possible to cite references or relegate the details to an appendix. The parametric interrelations presented here were used in designing the feasibility-model resonator and in selecting suitable diodes. The actual dimensions of that model and the parameters of its diodes are used in this section to illustrate the use of the design relations.

Some fundamental relationships for a symmetrically loaded, single-resonator filter are as follows:

$$Q_L \equiv f_0/\Delta f_3$$

$$\frac{2}{Q_E} \equiv \frac{1}{Q_L} - \frac{1}{Q_u}$$

where

$\Delta f_3 \equiv$ 3-dB bandwidth

$f_0 \equiv$ Resonant frequency.

Channel-center insertion loss, in dB, is

$$20 \log_{10} (Q_E/2Q_L)$$

or

$$20 \log_{10} [1 + (Q_E/2Q_u)]$$

or

$$20 \log_{10} [Q_u/(Q_u - Q_L)] \quad .$$

Channel-center input VSWR is $1 + (Q_E/Q_u)$. Accordingly, some subsidiary design objectives for the developmental single-resonator filter* were:

Loaded Q, Q_L	111 for $Q_u = 1000$ 125 for $Q_u \rightarrow \infty$
3-dB bandwidth, Δf_3	3.2 ± 0.4 MHz
Insertion loss at f_0	1.0 dB, maximum
Input VSWR at f_0	1.25, maximum.

B. Basic Resonator

Whereas Figure 3 shows the electrical essentials of the resonator to be modeled, the mechanical essentials are shown in Figure 4. The main resonator is coaxial, with diameters D_1 (inner) and D_2 (outer), and overall length 2ℓ. A series inductance is provided at each end by a radial-line stub (or trench) whose planar conductors have the spacing h.

---

*Having specified Q_E and Q_u for each resonator, corresponding design objectives for a multi-resonator filter with higher selectivity could be stated, whether the resonators would be simply cascaded, or multiply intercoupled as in an "elliptical-function" filter design. However, this was beyond the scope of the current contract.

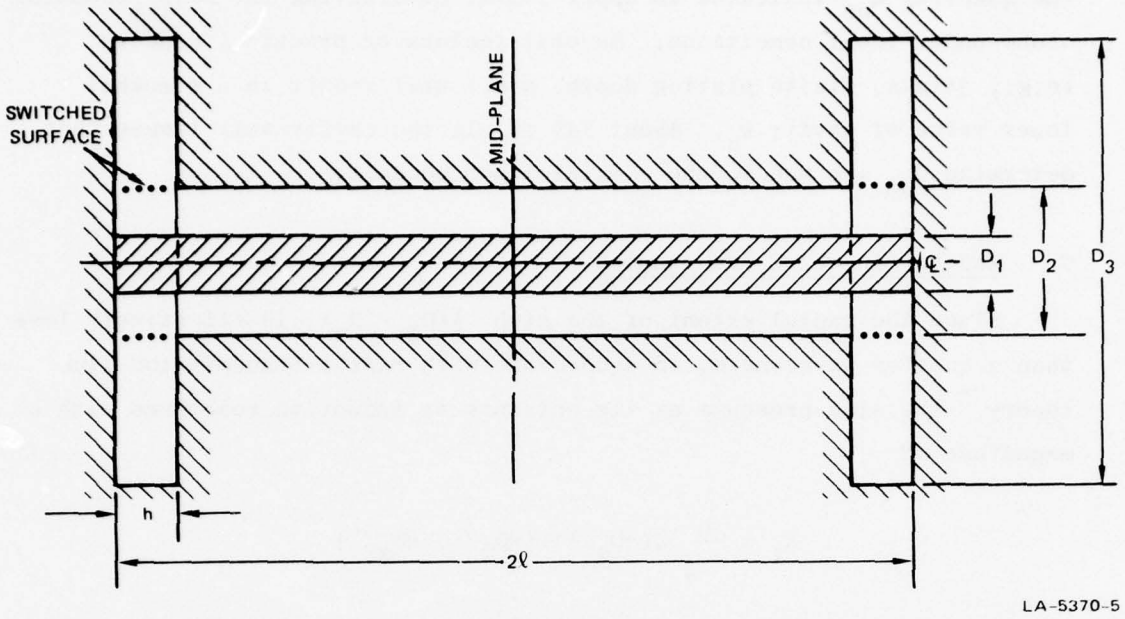

FIGURE 4 BASIC CONFIGURATION OF FEASIBILITY-MODEL FILTER RESONATOR

The radial line has its entrance at diameter D_2 and a short-circuit at diameter D_3. The dotted lines indicate surfaces that would, ideally, be made *conducting or nonconducting* through the use of PIN diodes.

For the main resonator (radial line stubs blocked off), one may write

$$Z_0 = 60 \ln (D_2/D_1) \text{ ohms}$$

and

$$Q_{u0} \equiv \frac{D_2/\delta}{\frac{D_2}{\ell} + \frac{1 + (D_2/D_1)}{\ln D_2/D_1}}$$

where δ is the skin depth appropriate to the frequency of interest. Since the actual design values of D_1, D_2, and ℓ are 1.00, 2.875, and 7.25 inches, respectively, $Z_0 = 63$ ohms and $Q_{u0} = 5440$, assuming $\delta = 1.3 \times 10^{-4}$ inch, which would apply for silver conductors at 370 MHz.

The quantity Q_{u0} indicates an upper limit, considering the main resonator alone under ideal conditions. Several factors of practical concern (e.g., joints, finite plating depth, etc.) will result in a somewhat lower value of cavity Q_u. About 74% of all the cavity wall losses that determine Q_{u0} are due to the coaxial inner conductor.

C. Radial-Line-Stub Inductances

Since the radial extent of the stub, $\frac{1}{2}(D_3 - D_2)$, is effectively less than a quarter wavelength, in accordance with radial-transmission-line theory,* the stub presents at its entrance an inductive reactance with a magnitude of

$$X_1 = -\frac{h}{\pi D_2} Z(\pi D_2/\lambda) T(\pi D_2/\lambda,\ \pi D_3/\lambda)$$

where the functions Z and T are evaluated as instructed in Ref. 3, and λ is the appropriate free-space wavelength. With actual design values of D_2, D_3 and h of 2.875, 10.05, and 0.75 inches, respectively, $X_1 \approx 11$ ohms for $\lambda \approx 33$ inches (i.e., ≈ 355 MHz).

This value of X_1 is, of course, only approximate because the configuration of the entrance to the radial line will, in practice, differ somewhat from the simple form shown when provision is made for mounting the PIN diodes and their biasing means.

The inductive radial-line section could also be realized by cutting inward toward the center of the inner conductor of the main coaxial cavity. In this case, the same reactance would be obtained with a relatively shallow notch. This approach was not attempted under the current contract, despite the overall compactness that would result, because difficulties in cooling and biasing the necessary diodes were anticipated for this configuration.

---

*See, for example, Ramo and Whinnery.[3] Figures 9.26 and 9.27 in the German Edition are especially useful.

D. Relation of Tuning Range to Stub Reactance

The subscripts A and B will be used to denote the lower and upper extremes of the tuning range, respectively. Neglecting any inductances associated with the closed switches (see Figures 3 and 4, stubs blocked off) as well as any loading due to the coupling probes, it is seen that the length ℓ is electrically $\pi/2$ at frequency f_{0B}. In consequence,

$$\frac{X_1}{Z_0} = \cot\left(\frac{\pi}{2}\frac{f_{0A}}{f_{0B}}\right)$$

if any capacitances associated with the open switches are neglected.* (At f_{0A} the resonator volume includes the space within the radial lines.)

From the above, for $f_{0A}/f_{0B} = 355/400 = 0.89$, X_1/Z_0 should ≈ 0.18. Thus, $X_1 \approx 11$ ohms should provide the requisite tuning range if $Z_0 = 63$ ohms for the main coaxial cavity. In practice, the residual inductance and capacitance of a switch are not altogether negligible. However, the effects produced are small enough to be accounted for with small correction factors. These correction factors are discussed in Appendix A and can be applied when more precision is desired.

E. RF Voltages and Currents in the Resonator

When a resonator has two coupling ports, each characterized by the same external Q, Q_E, the input power, P_0, appears magnified by the factor

$$\frac{2}{\pi} Q_E$$

with regard to any temporal or spatial maxima of RF voltage and current within the resonator.[4] Consequently, the peak RF voltage between the

*The derivation here uses basic theory applicable to end-loaded, lossless, uniform transmission lines.

conductors of the coaxial resonator at its mid-plane is*

$$\hat{V}_m = \left(\frac{4}{\pi} Q_E P_0 Z_0\right)^{\frac{1}{2}} \quad .$$

Correspondingly, the rms RF current at either end of the resonator is

$$\tilde{I}_e = \left(\frac{2}{\pi} Q_E P_0 / Z_0\right)^{\frac{1}{2}}$$

whether the switches are open or closed. For the numerical case being considered, $\tilde{I}_e \approx 50$ A. When the switches are closed, the current flowing through them would be $\tilde{I}_e$, assuming negligible switch inductance. When the switches are open, the peak RF voltage across the entrance of the radial line stub is

$$\hat{V}_A = \sqrt{2}\, \tilde{I}_e X_1 = \frac{X_1}{Z_0} \left(\frac{4}{\pi} Q_E P_0 Z_0\right)^{\frac{1}{2}}$$

or

$$\frac{X_1}{Z_0} \hat{V}_m$$

or

$$\cot\left(\frac{\pi}{2} \frac{f_{0A}}{f_{0B}}\right) \left(\frac{4}{\pi} Q_E P_0 Z_0\right)^{\frac{1}{2}} \quad .$$

Thus, $\hat{V}_A \approx 800$ V for the numerical case being considered.

---

*For the case $P_0 = 1000$ W, $Q_E = 250$, and $Z_0 = 63$ ohms, $\hat{V}_m \approx 4480$ volts. This estimate is relevant, for example, to the insulation requirements associated with coupling probes inserted near the cavity mid-plane.

F. Switch Stresses and Dissipation

So far, the term "switch" has been employed without specifying how PIN diodes would be used to constitute a switch. The use of back-to-back PIN-diode pairs, illustrated in Figure 5, is highly advantageous. The voltage stress per diode is halved, each diode is equally well provided with a heat sink, and bias can be applied to the center point of the pair without necessitating a bias choke because the bias lead shown lies along an equipotential of RF voltage. The two diodes are biased

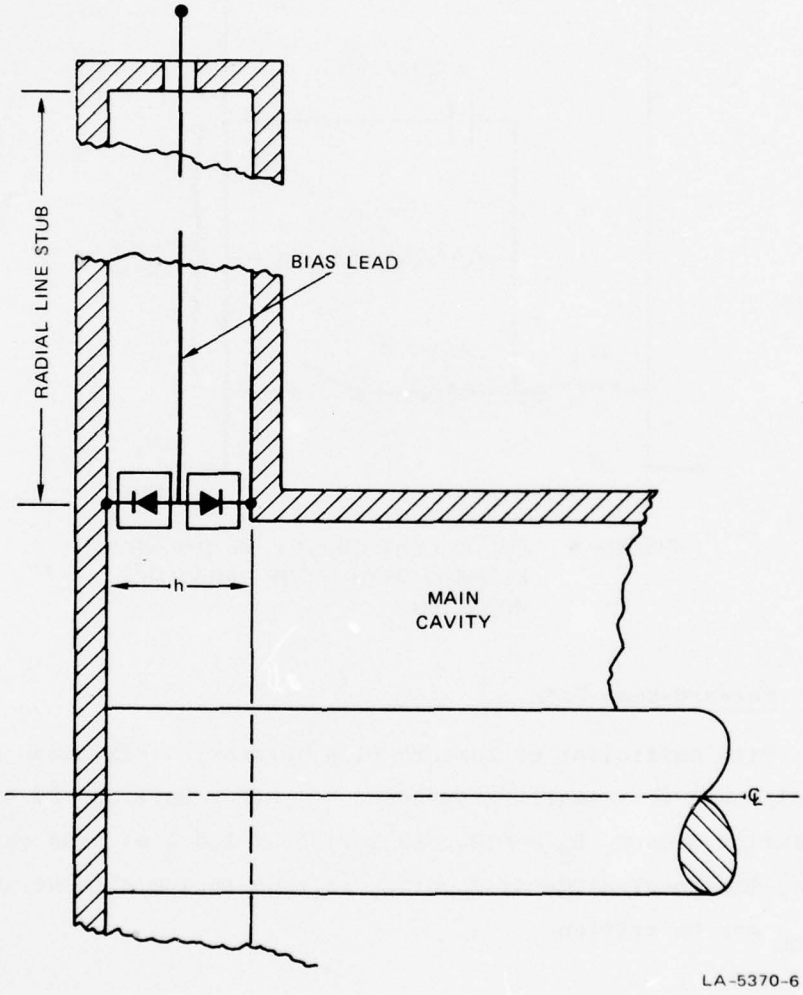

FIGURE 5 USE OF BACK-TO-BACK PIN-DIODE PAIR AS SWITCH ACROSS INDUCTIVE STUB

in parallel, but they are in series with respect to RF voltages and currents.* In addition, a number, n, of diode pairs is used in parallel, uniformly distributed around the circumferential entrance to the radial line. Figure 6 is an equivalent circuit representing an entire tuning element at UHF, with all diode parasitics included, but neglecting other sources of loss associated with the radial-line reactance.

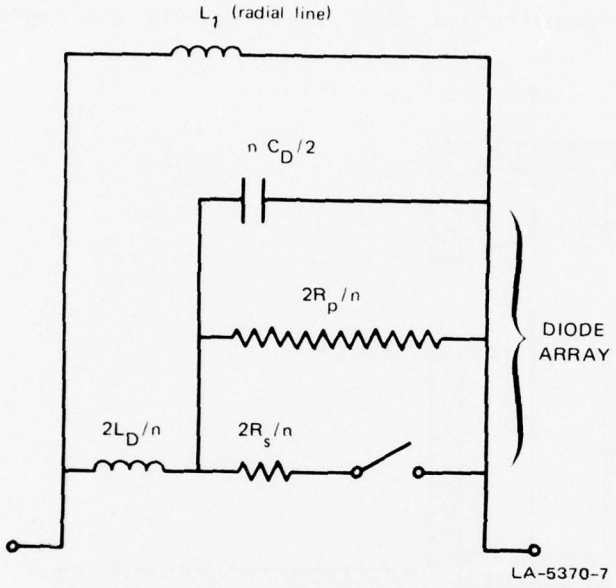

FIGURE 6 EQUIVALENT CIRCUIT OF TUNING ELEMENT WITH DIODE PARASITICS INCLUDED

1. Forward-Bias Case

With sufficient dc forward-bias current, a PIN diode acts essentially as a very small resistance, R_s. (For Unitrode UM 4000- and UM 4900-series diodes, $R_s \approx 0.05$ ohm for about 1.5 A of bias current.) Therefore, the total diode dissipation in each tuning element at frequency f_{OB} can be written

*This diode-pairing scheme is employed widely and in a variety of applications, such as the electronic tuning of coaxial magnetrons.[5]

$$P_{d1B} = \frac{2}{n} R_s \tilde{I}_e^2$$

and the thermal stress per diode is

$$P_{dDb} = R_s(\tilde{I}_e/n)^2 \quad .$$

The quantity P_{d1B} is used in expressing the overall resonator Q_u at f_{0B}, or Q_{uB}. The quantity P_{dDB} is to be compared against the dissipation rating of the diode (e.g., 25 W for a UM 4000C, or 37 W for a UM 4900C, assuming a heat-sink temperature of 25°C.)

2. Reverse-Bias Case

A reverse-biased PIN diode is conveniently represented as a capacitance (≈ 3 pF maximum for the diode types considered here) shunted by a resistance, R_p, that accounts for all the associated RF losses. The value of R_p exhibits a dependence on frequency, bias voltage, and in some cases, the RF voltage applied. Near 350 MHz, R_p values of about 70,000 ohms can be obtained for UM 4000 and UM 4900 diodes at a dc reverse bias in excess of a few hundred volts.

The peak RF voltage stress per diode is clearly

$$\hat{V}_1 = \tfrac{1}{2}\hat{V}_A$$

or ≈ 400 V for the numerical case being considered--i.e., for P_0 = 1000 W, Q_E = 250, Z_0 = 63 ohms, and $X_1 \approx 11$ ohms. The thermal stress per diode is then (at frequency f_{0A})

$$P_{dDA} = \tfrac{1}{2}\hat{V}_1^2/R_p \quad .$$

However, since P_{dDA} is, in practice, smaller than P_{dDB}, it is of minor importance. The total diode dissipation in each tuning element at frequency f_{0A} is

$$P_{d1A} = n\hat{V}_1^2/R_p \quad ,$$

a factor needed for the determination of Q_{uA}. It is important to note that P_{d1A} (total diode dissipation for reverse bias) is proportional to n, whereas P_{d1B} (for forward bias) is inversely proportional to n. Also, P_{dDA} (dissipation per diode for reverse bias) is independent of n, but the more-significant P_{dDB} (per diode for forward bias) is inversely proportional to n^2.

Attention is directed to the fact that P_0 and Q_E appear only as a product in all expressions for the currents, voltages, and dissipations associated with the diodes and other internal resonator elements. Consequently, tradeoffs between input power and external loading are permissible without affecting the drives on the internal elements. For example, the diodes would be unaffected if the input power and the loaded bandwidth were both multiplied by the same factor.

G. Calculation of Unloaded Q

From a systems viewpoint, unloaded Q is an important measure of resonator performance. Expressions for Q_{uA} and Q_{uB} that account for both diode and cavity-wall dissipation are required. The derivations are given in Appendix B, with the results presented and discussed below. It should be noted that at f_{0B}, energy is stored only in the main resonator, while at f_{0A} it is stored in the reactance X_1 as well. Energy storage in diode inductances or capacitances may be neglected.

The quantities $Q_{u\ell A}$ and $Q_{u\ell B}$, sometimes referred to as cavity Q_u, designate the values of Q_{uA} and Q_{uB} obtainable if lossless diodes ($R_s \rightarrow 0$ and $R_p \rightarrow \infty$) were installed in the resonator. That is, all dissipative contributions are accounted for by $Q_{u\ell A}$ and $Q_{u\ell B}$ except those occurring within the PIN chips. Exact values of $Q_{u\ell A}$ and $Q_{u\ell B}$ are thus not readily predictable, though from experience they might be expected to be between 60% and 80% of Q_{u0}. However, experimental determination is possible using a technique based on "dummy" diodes, as described in Section V-A-1.

In this way, any effects due to bias adjuncts, joints in the cavity walls, or "current crowding" (i.e., nonuniformities in RF wall currents concentrating near diode installation points) are taken into account.

1. Forward-Bias Case

Just as $Q_{u\ell B}$ designates the value of Q_{uB} with lossless diodes and an actual resonator, Q_{u1B} is defined as the value of Q_{uB} with actual diodes and a lossless resonator. Then,

$$\frac{1}{Q_{uB}} = \frac{1}{Q_{u\ell B}} + \frac{1}{Q_{u1B}}$$

where

$$Q_{u1B} = n\pi Z_0/8R_s$$

as derived in Appendix B. For reference, Figure 7 shows the dependence of Q_{uB} on $Q_{u\ell B}$ for the case of $R_s = 0.05$ ohm, $Z_0 = 63$ ohms, and $n = 6$, 8 or 10. It is apparent that with sufficiently large resonator diameters, diode losses predominate, while with small diameters, cavity losses predominate.

2. Reverse-Bias Case

As noted, $Q_{u\ell A}$ is the value of Q_{uA} for lossless diodes in an actual resonator. However, since energy storage is now possible in the reactance X_1, there is a "tuning element Q" defined by

$$Q_{XA} \equiv 2R_p/nX_1 \quad .$$

Consequently,

$$\frac{1}{Q_{uA}} = \frac{1}{KQ_{XA}} + \frac{1}{Q_{u\ell A}}$$

where

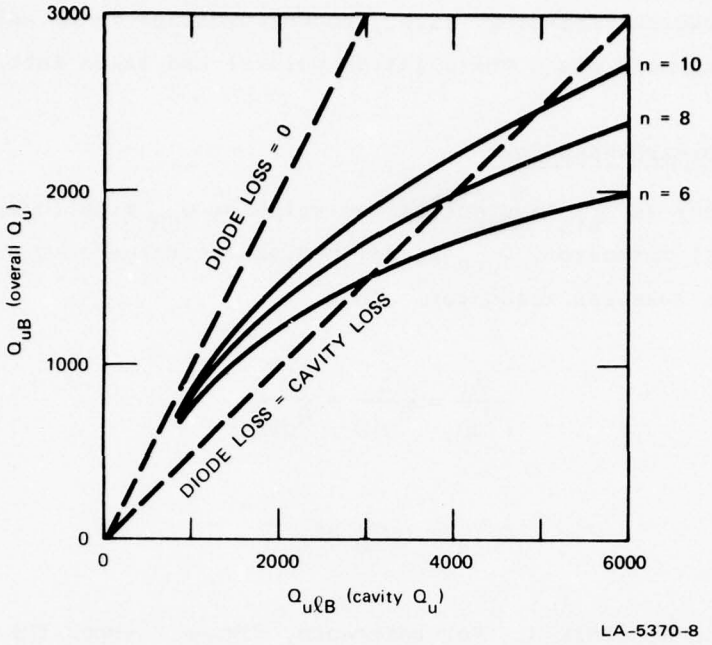

FIGURE 7 DEPENDENCE OF OVERALL Q_u ON CAVITY Q_u FOR Z_0 = 63 ohms AND TUNING ELEMENTS HAVING n PAIRS OF FORWARD-BIASED DIODES FOR WHICH R_s = 0.05 ohm

$$K \equiv 1 + \frac{\pi}{4} \frac{f_{0A}}{f_{0B}} \frac{Z_0}{X_1}$$

as derived in Appendix B. Thus, the asymptotic values of Q_{uA} are $Q_{u\ell A}$ (lossless diodes) and $Q_{u1A} \equiv KQ_{XA}$ (lossless cavity). Corresponding to Figure 7, Figure 8 shows the dependence of Q_{uA} on $Q_{u\ell A}$ for the case f_{0A} = 355 MHz, f_{0B} = 400 MHz, Z_0 = 63 ohms, X_1 = 11 ohms (whence $K \approx 5$), R_p = 70,000 ohms, and n = 6, 8 or 10.

H. Optimum Number of Diode Pairs in Parallel

For the feasibility model constructed, the number, n, of diode pairs in parallel per tuning element was chosen to be 6. After thorough testing (Section V) had provided reliable values of R_s, R_p, $Q_{u\ell A}$, and $Q_{u\ell B}$, use of Figures 7 and 8 disclosed that n = 10 would have been the

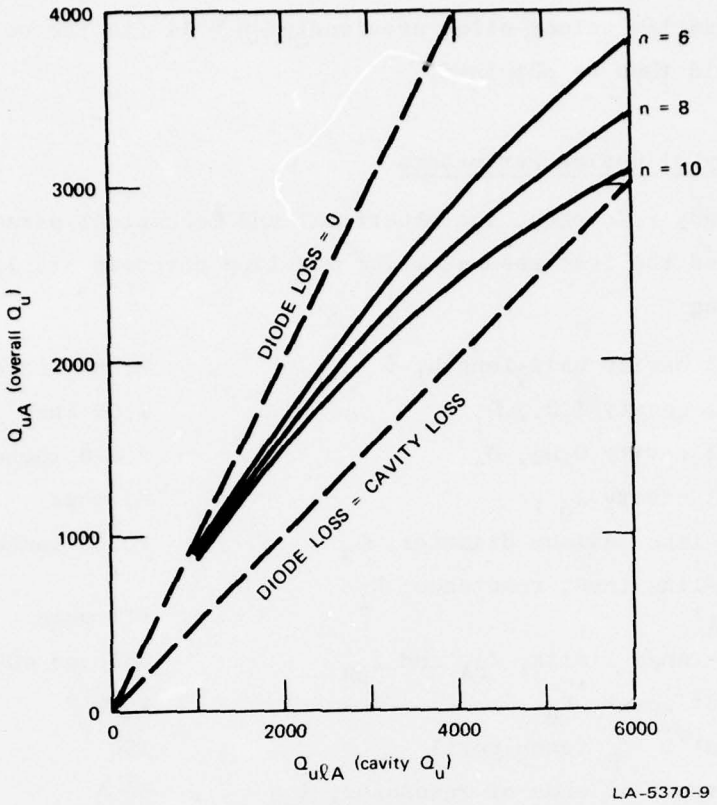

FIGURE 8 DEPENDENCE OF OVERALL Q_u ON CAVITY Q_u FOR Z_0 = 63 ohms AND TUNING ELEMENTS GIVING f_{0A}/f_{0B} = 0.89 AND HAVING n PAIRS OF REVERSE-BIASED DIODES FOR WHICH R_p = 70,000 ohms

optimum choice, though somewhat more costly. The relevant criterion is that $Q_{uA} \approx Q_{uB}$, whereby a maximum value of Q_u is obtained for the entire tuning range.

For possible preliminary design purposes, one might wish to attempt a rough estimation of the optimum value of n by ignoring stored energy differences and losses other than those in the diode chips. In this case, $Q_{uA} = Q_{uB}$ reduces to $P_{d1A} = P_{d1B}$, whence

$$n = \frac{2(R_s R_p)^{\frac{1}{2}}}{Z_0} \tan\left(\frac{\pi}{2}\frac{f_{0A}}{f_{0B}}\right) \quad .$$

For the parameter values cited previously, n = 11 (to the nearest whole number) would then be obtained.

I Summary of Design Parameters

For ready reference, the electrical and mechanical parameters that characterized the test resonator for modeling purposes are listed in the following:

Coaxial cavity half-length, ℓ	7.38 inches*
Coaxial cavity I.D., D_1	1.00 inch
Coaxial cavity O.D., D_2	2.875 inches
Coaxial cavity Z_0	63 ohms
Radial-line maximum diameter, D_3	10.05 inches
Radial-line input reactance, X_1 (at f_{0A})	+11 ohms
Tuning-range limits, f_{0A} and f_{0B}	355 and 400 MHz
RF input power, P_0	1000 W
External Q, Q_E (each port)	250
RMS current at ends of resonator, $\tilde{I}_e$	50 A
Peak voltage at mid-plane of resonator, $\hat{V}_m$	4480 V
Peak voltage across radial line entrance, $\hat{V}_A$	800 V
Peak voltage stress per diode, $\hat{V}_1$ (at f_{0A})	400 V
PIN diode type	UM 4000 series
Number of diode pairs in parallel, n	6
Maximum diode capacitance, C_D	3 pF
Minimum net diode reactance (at f_{0A})	-50 ohms
Diode inductance, L_D	$\rightarrow$ 0
RMS RF current per diode (at f_{0B})	8.33 A

*Actual mechanical dimension is 7.25 inches.

Diode "dynamic" forward resistance, R_s	0.05 ohm*
Diode equivalent reverse shunt resistance, R_p	70,000 ohms*
Diode dissipation at f_{0A}	
Per diode, P_{dDA}	1.1 W
Per tuning element, P_{d1A}	13.7 W
Diode dissipation at f_{0B} †	
Per diode, P_{dDB}	3.5 W
Per tuning element, P_{d1B}	41.7 W
Upper limit for cavity Q_u, Q_{u0}	5440
At f_{0A}: Q_u with no diode losses, $Q_{u\ell A}$	3260‡
At f_{0A}: Q_u with only diode losses, Q_{u1A}	10610
At f_{0A}: Overall Q_u, Q_{uA}	2490
At f_{0B}: Q_u with no diode losses, $Q_{u\ell B}$	3715‡
At f_{0B}: Q_u with only diode losses, Q_{u1B}	2970
At f_{0B}: Overall Q_u, Q_{uB}	1650

*Values best fitting experimental data.

†Not including forward-bias power.

‡Experimentally determined (Section V-A-1).

IV FEASIBILITY MODEL DESIGN AND CONSTRUCTION

A. General

Figure 9 shows the filter model developed and evaluated under the current contract. The center section is the coaxial main resonator, which is penetrated by the input and output coupling probes (with type-N coaxial connectors). The radial-line tuning element at each end is flanked by natural-convection aluminum cooling fins for evacuating the heat developed within the tuning element so that excessive diode temperatures will not occur under CW operation. Terminals for applying bias to the 12 diodes internal to each tuning element are also visible in the photograph.

No effort was made to reduce the volume of this mechanical model because the primary purpose was to demonstrate electrical feasibility.* However, as a result of having fully evaluated this model, the physical form of possible future developments can be predicted fairly realistically. For example, all the transverse dimensions of the present resonator could readily be halved, with only a small effect on the filter performance. Cavity losses would increase (predominantly in the inner conductor of the coaxial section), but not the diode losses, and the insertion loss would rise by only a few tenths of a dB. The power density for cooling purposes would be increased somewhat, but certainly not excessively.

---

*The decision to limit the radial-line width, h, to 0.75 inch requires justification, because the choice of a larger value of h would have resulted in a smaller value of D_3 and a much smaller overall volume for the resonator. As may be seen in Figure 2, an eventual multichannel resonator would require several radial-line inductances (of the same design), some of which would have to be quite close together in the vicinity of the resonator mid-plane. Considering this situation, 0.75 inch is the maximum allowable value for h in resonators operating near 400 MHz.

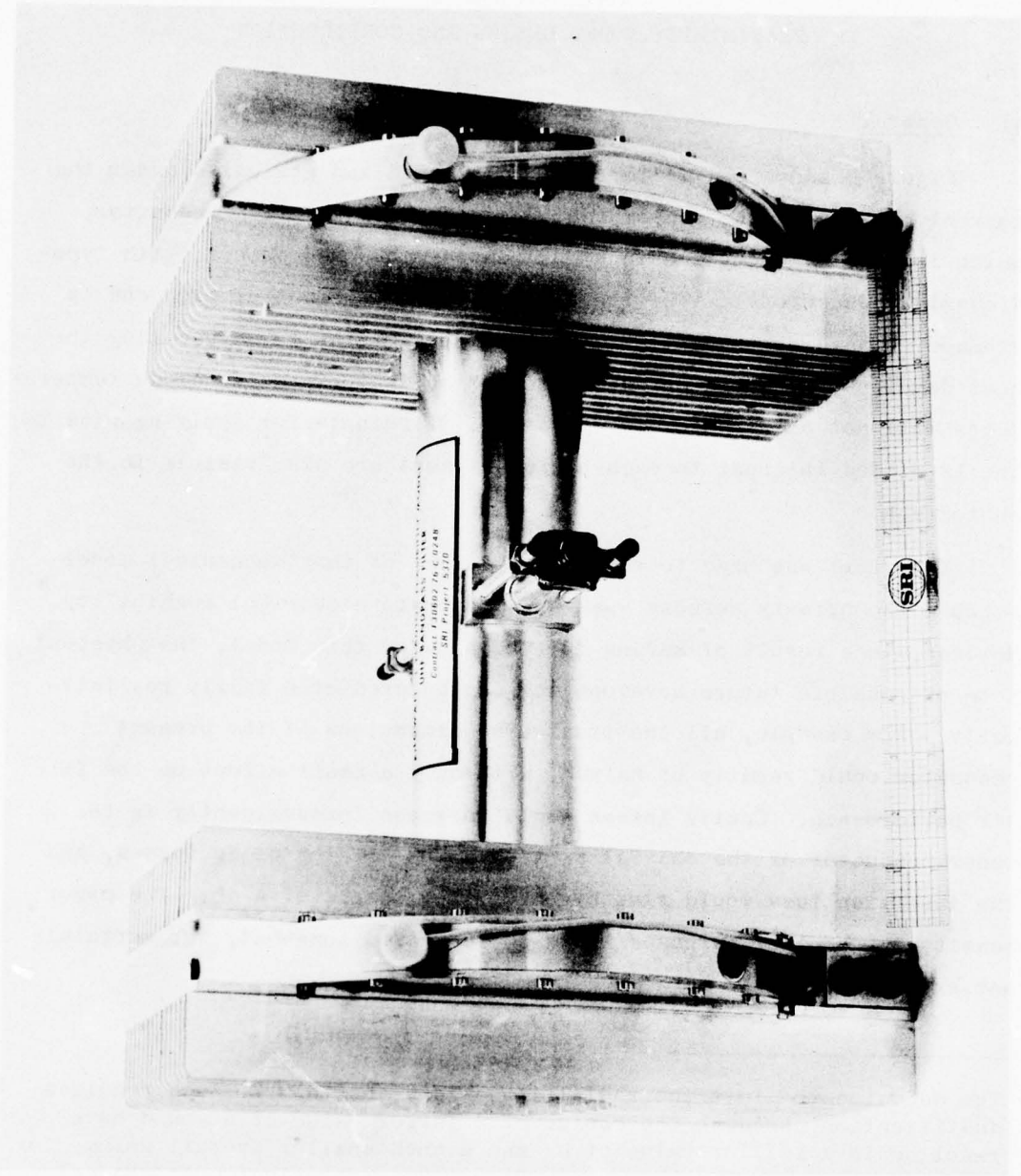

FIGURE 9 DEVELOPMENTAL FEASIBILITY MODEL OF HIGH-POWER UHF BANDPASS FILTER WITH L-TYPE ELECTRONIC TUNING

For convenience, the principal material used was brass, silver-plated to a thickness of several skin depths. To minimize losses at joints, all flanges were designed so that a large contact pressure would exist at these joints. Many of the design details were predicated on the choices made regarding the requisite array of PIN diodes, discussed in the next section.

B. Diode Selection

From the design relations it became evident that a resonator having reasonable values for Z_0 and n and meeting the requirements for Q_u and tuning range would be possible only if diodes with $R_s < 0.1$ ohm were procurable. Only Unitrode series UM 4000 and UM 4900 diodes were known to quality. Moreover, it appeared likely that $R_s \approx 0.05$ ohm might be obtained for these diodes at a forward-bias current between 1.5 and 2.0 A. It also appeared that R_p values for these diodes for frequencies near 350 MHz (and several hundred volts of reverse bias) would be sufficiently large.

As for diode capacitance under reverse bias, the modeling relationships (Section III-D and Appendix A) indicated that the influence of the relatively large capacitances of a UM 4000 or UM 4900 diode (2.6 pF, typical; 3.0 pF, maximum) would be neither critical nor excessive, even when several diode pairs were paralleled. The UM 4000 and UM 4900 contain the same PIN chip, but in the costlier UM 4900 the chip lies closer to the heat sink so its thermal resistance is lower--4°C/W instead of 6°C/W for the "C" package. However, since the thermal stresses per diode in the present resonator design are quite modest, relative to what is allowable, Series UM 4000 C diodes were chosen.* Since peak RF voltages per diode in the range of 400 to 450 V were anticipated for 1000 W of RF input power to the resonator, Type UM 4010 C, assigned a

---

*Since diode inductance is of little concern in the current work, the slightly reduced inductance provided by the shorter package of the UM 4900 C offers no advantage.

minimum voltage rating of 1000 V by the manufacturer, was selected.* In a batch of thirty UM 4010 C diodes, all but four exhibited room-temperature leakage currents of 0.5 μA or less, and in some cases only 0.1 μA, at 600 V. For this group, 2 V_R (1 μA) values of roughly 1600 V minimum can be estimated.†

Two sets of 12 diodes each were selected from these 26 for installation in the two tuning elements of the resonator. Since the 12 diodes in each set were to be biased in parallel, dc forward resistances were measured at fixed bias currents so that diodes having most nearly the same dc forward resistance would be in the same set. (The corresponding dc voltage drop is typically 0.9 V at 1.0 A per diode and will increase only to 1.0 V at 2.5 A per diode.)

C. Resonator Details

Figure 10 indicates the arrangement and essential dimensions of the main (coaxial) cavity and of a radial-line inductance. For the coaxial section, Z_0 = 63 ohms, and the resonant frequency would be 407.3 MHz if the radial lines were totally blocked off. The input reactance of each radial line is about 11 ohms at 355 MHz. Six pairs of UM 4010 C PIN diodes are uniformly distributed around the entrance of each radial line section.

---

*The manufacturer's rating, V_R(10 μA), defined as the lower limit of the reverse voltage yielding a leakage current of 10 μA at 25°C, may not be sufficiently informative in the case of "soft-knee" PIN diodes. SRI's practice, therefore, is to ascertain the approximate value of V_R (1 μA) at room temperature for each diode in a shipment. Then, the maximum allowable sum of the bias and peak RF voltages for the diode (the effective "breakdown" voltage) would be 2 V_R(1 μA).

†The 1600-V value implies a possible RF input power rating for the filter resonator as high as 4 kW, CW. With other diodes, selected for 2 V_R(1 μA) = 2000 V, some of which can be found in every production lot, P_0 could be raised to over 6 kW and dissipation ratings would still not be exceeded under CW operation.

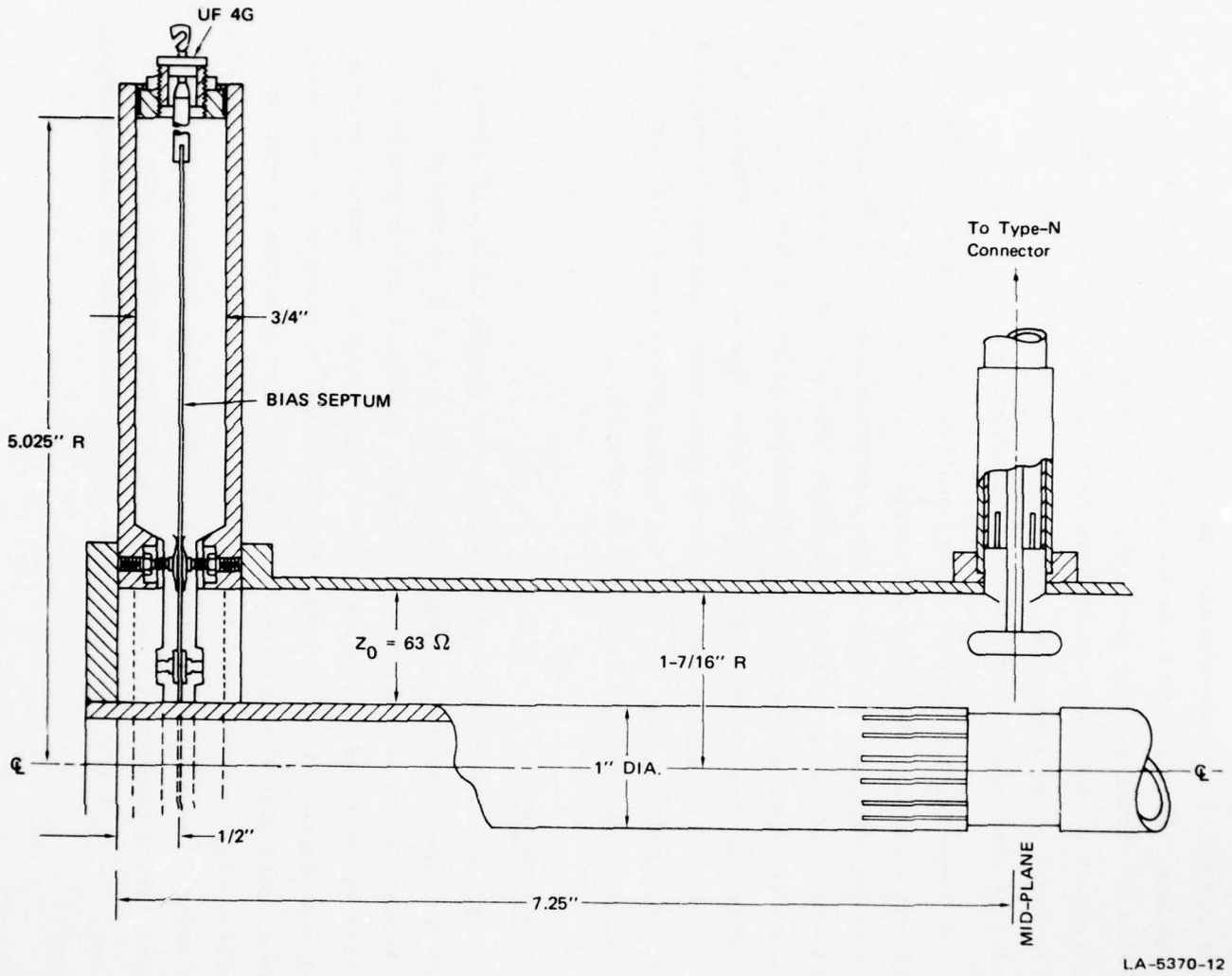

FIGURE 10 ESSENTIAL CONFIGURATION OF DEVELOPMENTAL ELECTRONICALLY TUNED UHF FILTER RESONATOR

The mounting for each diode was arranged to facilitate the removal of heat from the cathode end of each diode, as illustrated in Figure 11. The thick base plate of each aluminum cooling-fin unit (Wakefield type 4509) was positioned to minimize the thermal resistances between it and the diodes. Thermalcote paste was used to assure thermal contact between the brass and the aluminum. At 1000 W of RF input power to the resonator, the power to be dissipated on either side of each diode array could be as much as 35 W ($\approx 6\ P_{dDB}$ + forward bias power), not including some nearby cavity-wall dissipation.

A large fraction of the cavity-wall dissipation (total $\approx$ 70 W maximum) occurs in the inner conductor of the coaxial section, tending to concentrate near the ends of the conductor due to the RF-current distribution pattern. Elevated temperatures are tolerable for the inner conductor, especially since a sliding joint (needed to facilitate assembly) is used at the center of the span (Figure 10). However, it was decided to cool the ends of the hollow inner conductor by inserting a finned aluminum plug, so that the nearby diodes would not receive any additional heat through radiation or convection.

D. Bias Means

As indicated in Figures 10 and 11, the anodes of all 12 diodes in each set are connected by means of a thin, flat disk or septum. The disk lies in the mid-plane of the radial line such that negligible perturbation of the RF fields in this region occurs. Contact between the bias septum and each diode is established by means of a low-inductance, gold-plated beryllium-copper spring that provides a positive, axial contact force of one to two pounds. (Up to 40 pounds is allowable if there is no transverse component.) One of the justifications for using spring contacts is the variation of diode height within a batch. Since $R_s \approx 0.05$ ohm, the allowable contact resistance is correspondingly minute.*

*Contacts of silver-bearing silicone elastomer were considered, but an excessive resistance increment was predicted. Soldered contacts would be electrically ideal, but diode breakage might result if sliding were prevented during mechanical shock or differential expansion of the parts.

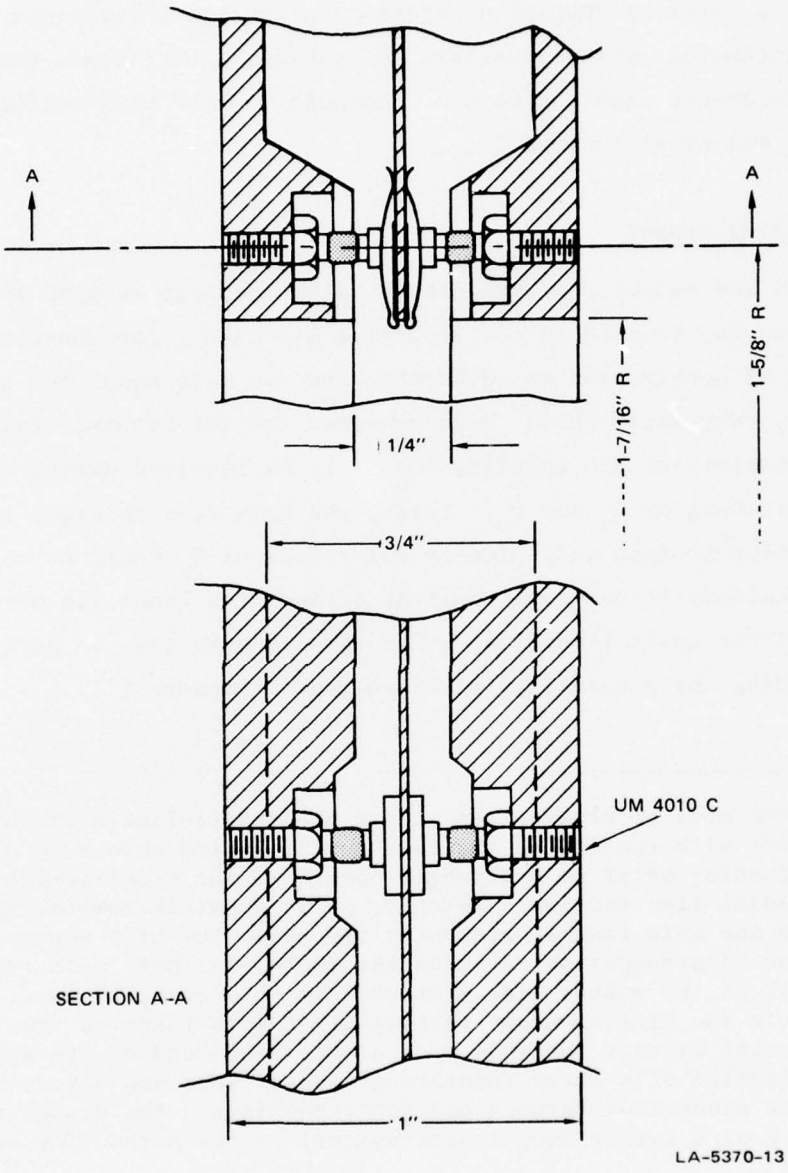

FIGURE 11 CONSTRUCTIONAL DETAILS IN VICINITY OF A DIODE PAIR

The bias septum is supported and centered by three bias feedthroughs (USSC/Centralab type UF4G), rated at 1000 Vdc, and installed in the outer rim of the radial line. Since the feedthroughs are electrically in parallel, a total of 9000 pF of bypass capacitance is provided as a simple precaution against possible RF leakage.* (In future work, different components might be chosen, depending on the bias-switching circuitry and other factors.)

E. Coupling Probes

Input and output coupling probes of the capacitive type (Figure 11) were chosen and located in the resonator mid-plane, for convenience.† The depth of penetration is adjustable and was made equal for both probes. Initially, very small "hats" were provided for the probes. This was useful when minimizing the coupling ($Q_E \rightarrow \infty$), as required during some of the measurements of Q_u and f_0. Later, the hats were enlarged to 0.75-inch diameter so that sufficiently low values of Q_E could be obtained with the hat positioned about halfway between the inner and outer conductors of the coaxial section. (The details here are, in part, concerned with avoiding any possibility of RF-voltage breakdown.)

---

*The desired mode of propagation within the radial-line section is an "even" mode with respect to the thin septum, which should be electrically neutral insofar as it is everywhere normal to the electric-field lines in the radial-line section. However, it is possible for the RF electric fields in the main coaxial resonator to excite the bias septum in an "odd" mode of propagation in which the septum is "hot" with respect to both walls of the radial line section. In this case, RF power could be lost via the biasing means unless action were taken to create a virtual short circuit for this mode at the diode end of the septum. The combination of a large feedthrough capacitance and a very-low-inductance connection between the feedthroughs and the diodes (as provided by a disk rather than a wire spider) is one method for effecting this.

†Some out-of-band leakage from input to output is possible here; due to their proximity, the small capacitance between the two probes is not entirely negligible. This effect is inconsequential as regards the project objectives.

An apparent property of this type of probe and coupling configuration is that Q_E is more frequency-dependent than would be the case for coupling loops. In the present model, a variation in Q_E from 320 at 350 MHz to 230 at 391 MHz was obtained for a fixed insertion depth. As regards the project objectives, the consequences of this variation are slight, especially since $\hat{V}_1 \propto \sqrt{Q_E}$.

V LOW-POWER TEST RESULTS

A. Weak External Coupling

1. Dummy Diodes Installed

Upon completing the fabrication and assembly of the developmental resonator model, testing was undertaken with milliwatt levels of RF input power. Initially, the coupling probes had small hats and minimal insertion, the better to measure resonant frequency, f_0, and unloaded Q, Q_u. Most importantly, the first tests were made with dummy diodes of solid metal having the same form as a Series UM 4000 C diode (Figure 12). Thus, all circuit effects were manifested except for the losses within the PIN chips. To make measurements where the actual reverse-biased diodes would be capacitors, a suitable thickness (0.003 inch) of Teflon tape is inserted between the cap of the dummy diode and the contact spring to produce a capacitance of 2.6 to 3.0 pF. Since the dummy diodes require no bias, it was possible to make measurements with and without the "bias hardware" installed. No effect on Q_{uA} (the parameter most likely to be affected) was observable.

The data obtained from these tests are as follows:

Tuning Case*	f_0, MHz	Q_u†
RR	f_{0A} = 358.35	$Q_{u\ell A}$ = 3260 ± 4%
FR	376.38	3420
FF	f_{0B} = 399.25	$Q_{u\ell B}$ = 3715 ± 2%

*The abbreviations indicate the following: RR--all diodes in reverse-bias state; FF--all diodes in forward-bias state; FR--one set of diodes in one state and the other set in the other state.

†The preferred method of measuring Q_u relies on a swept-frequency, polar-display (Smith chart) network analyzer. More precision is usually obtained than when Q_u is inferred from measurements (footnote continued)

PRECEDING PAGE BLANK-NOT FILMED

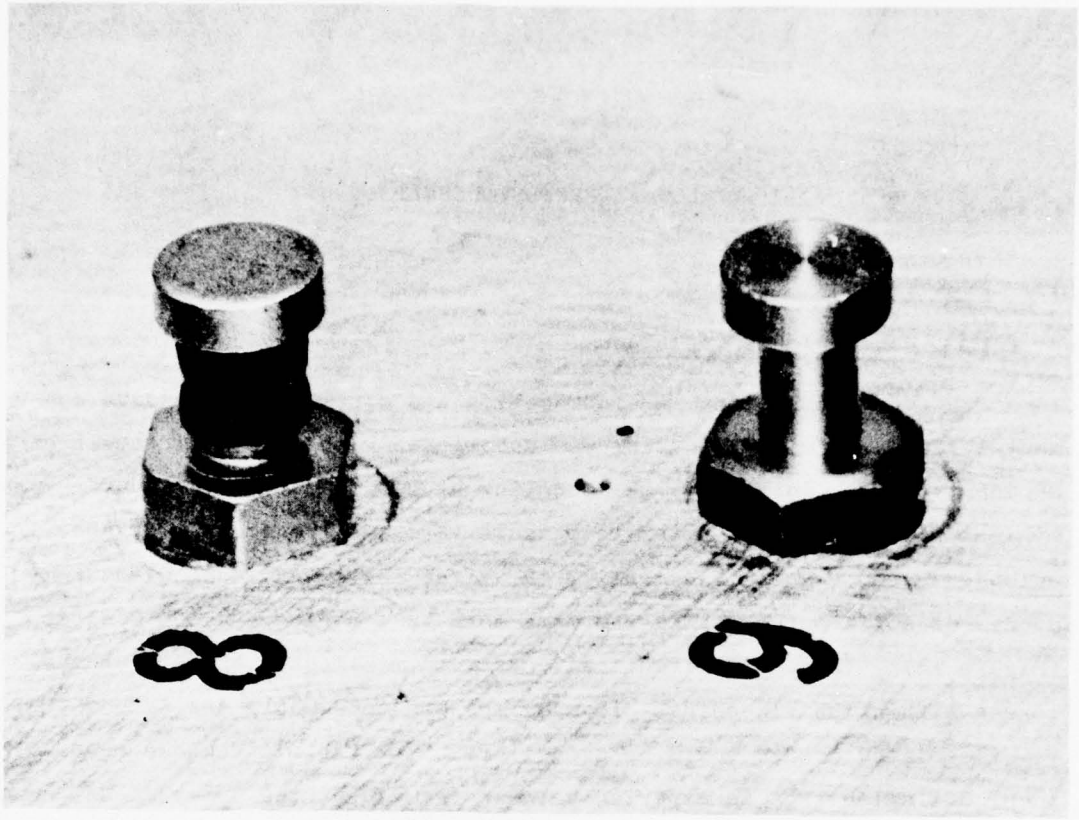

FIGURE 12 *UNITRODE UM 4010 C PIN DIODE (left) AND BRASS "DUMMY"* (right) SCREWED INTO A HEAT-SINK PLATE. Hex nut size is 4-40.

It is thus seen that about 41 MHz of tuning range (11%) has been obtained. Also, $Q_{u\ell A}$ and $Q_{u\ell B}$, which are effective Q_u values with all sources of loss represented except those occurring internal to the diodes, range from 58% to 71% of the Q_{u0} applicable to an ideal, silver, coaxial resonator at the appropriate frequencies. Evidently, $Q_{u\ell A} < Q_{u\ell B}$, because at f_{0A} the extended cavity effectively has a less advantageous surface-to-volume ratio.

(footnote continued) of filter insertion loss and bandwidth. A single coupling probe is used, with minimal insertion, and the parameter $\vec{S}_{11}$ is displayed. A frequency counter is used to measure precisely the frequencies for which the $\vec{S}_{11}$ locus intersects certain reference lines added to the display screen. The method is described elsewhere.[6]

2. Actual Diodes Installed

When the dummy diodes were replaced with actual diodes, and bias applied, the test data obtained were as follows:

Tuning Case	f_0, MHz	Q_u
RR	f_{0A} = 357.6 MHz	Q_{uA} = 2565
FR	377.0	2020
FF	f_{0B} = 401.6 MHz	Q_{uB} = 1700

These Q_u values do, of course, depend on the bias magnitudes. The data above apply when the forward-bias current is 1.5 A per diode (18 A per tuning element) and when the reverse bias voltage $\geq$ 250 V. The value of Q_{uA} increases with reverse-bias voltage, but ceases to change beyond about 250 V, and Q_{uA} = 2565 is the "saturation" value. The value of Q_{uB} increases with forward-bias current as shown in Figure 13. As indicated, improvement is possible beyond Q_{uB} = 1700 at 1.5 A, but it is small. The small changes in f_{0A} and f_{0B} that occurred upon replacing dummy diodes with actual diodes imply that the actual diodes effectively have slightly more capacitance and less inductance than do the dummies. The data obtained for Tuning Case FR were intermediate in value, as one would expect. Due to the mechanical and electrical symmetry, the data observed for this tuning case are indifferent to which end of the resonator is "F" and which is "R".

Referring to Figure 7, with $Q_{u\ell_B} \approx 3715$ and n = 6, it is seen that the final value of Q_{uB} = 1700 is quite consistent with the assumption of R_s = 0.05 ohm, insofar as the modeling relations of Section III-G-2 are exact. Accordingly, this value of R_s represents an average for a particular batch of 24 diodes (observed near 400 MHz).* Figure 7 also indicates that at f_{0B}, diode losses and cavity wall losses are roughly balanced in the present resonator model.

*According to the manufacturer, there is considerable variation in the curves of R_s versus bias current from diode to diode and batch to batch, especially when $R_s < 0.1$ ohm. However, R_s = 0.05 ohm at 1.5 A is within the anticipated range.

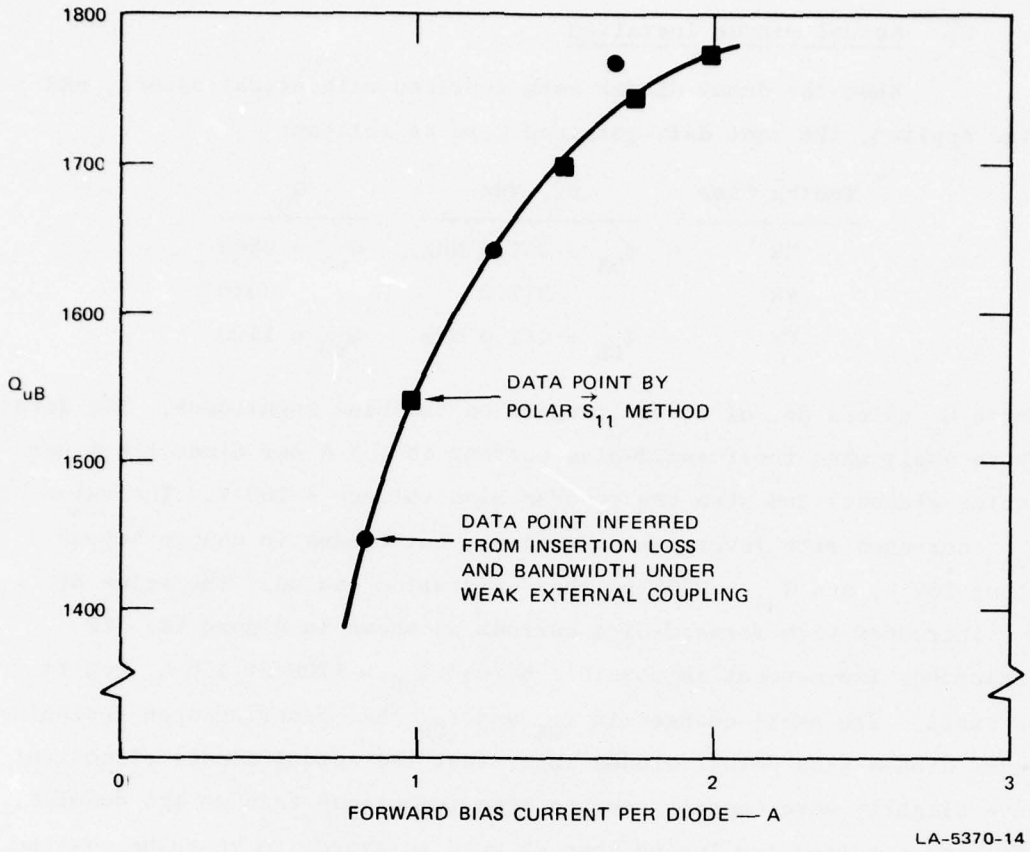

FIGURE 13 VARIATION OF OVERALL Q_u WITH BIAS CURRENT AT f_{0B} = 401.6 MHz

Referring to Figure 8, with $Q_{u\ell A} \approx 3260$ and n = 6, the final value of Q_{uA} = 2565 is seen to be consistent with the assumption of R_p = 70,000 ohms, insofar as the modeling relations of Section III-G-3 are accurate. This value of R_p is thus an effective average for the 24 diodes installed, for the frequency ($\approx$ 360 MHz) and bias indicated.*

*Manufacturer's published data on R_p are difficult to interpolate, with respect to frequency, or to extrapolate, with respect to bias voltage. Hence, $R_p \approx 50{,}000$ ohms was the best estimate available prior to testing SRI's resonator. However, SRI was advised that, according to the limited testing done at the factory, recently made batches of diodes were exhibiting higher values of R_p than those published.

Figure 8 also indicates that at f_{0A}, cavity-wall losses predominate over diode losses in determining Q_{uA} for the present resonator model.

Assuming that the indicated values of R_s and R_p are maintained by the manufacturer, it is of interest to predict the effects of halving all the transverse dimensions of the present resonator in order to reduce bulk in a possible future model. $Q_{u\ell A}$ and $Q_{u\ell B}$ should then drop to about 1600 and 1800, respectively. Figures 8 and 7 then predict Q_{uA} and Q_{uB} values for n = 6 of about 1400 and 1100, respectively, or, for n = 8, about 1300 and 1250, which are sufficiently close to equality. The filter insertion loss would, accordingly, increase from 0.5 or 0.6 dB only to about 0.8 or 0.9 dB, with cavity wall losses (largely due to the inner conductor of the coaxial section) predominating somewhat over diode losses.

B. Strong External Coupling

The feasibility-model filter was completed by enlarging the coupling-probe hats and inserting the probes (symmetrically) to obtain the desired value of Q_E for each of the two ports. Since Q_E was found to be frequency-dependent, the objective was to bring the mean of Q_{EA} and Q_{EB} to roughly 250, whereupon the probes were locked in position. The resonator was then tested as a bandpass filter with three possible tuning channels. The performance data summarized in Table 1 apply for low levels of RF power, a forward-bias current of 1.5 A per diode, and nominal reverse-bias voltages > 250 V. The enlarged coupling probes capacitively loaded the resonator significantly, so that the entire tuning range was shifted downward in frequency.

Table 1

PERFORMANCE DATA OF FEASIBILITY MODEL BANDPASS FILTER

Parameter	Tuning Case RR*	Tuning Case FR	Tuning Case FF†
Probes Retracted			
Resonant frequency, MHz	357.6	377.0	401.6
Measured unloaded Q, Q_u	2565	2020	1700
Probes Inserted			
Channel center frequency, MHz	349.8	368.0	391.0
Observed 3-dB bandwidth, MHz	2.3 ± 0.1	2.92 ± 0.08	3.63 ± 0.08
Loaded Q, Q_L	152	126	108
Computed external Q, Q_E	323	269	231
Insertion loss			
Predicted from above Q_u and Q_L, dB	0.53	0.57	0.58
Measured (all ±0.05), dB	0.52	0.59	0.62
VSWR at f_0			
Computed from Q values	1.126	1.133	1.136
Measured	< 1.15	< 1.15	< 1.15
VSWR at edges of 3-dB bandwidth	≈ 7	≈ 7	≈ 7

*Indicated by subscript A in Section III.

†Indicated by subscript B in Section III.

VI HIGH-POWER TEST RESULTS

To complete the experimental program for the current contract, the feasibility-model filter was operated, without any signs of overloading, at RF input power levels up to 1250 W, CW, the maximum obtainable from the transmitter used. During this operation only modest temperature rises resulted, accompanied by a downward drift of about 350 kHz in resonant frequencies. Otherwise, to within the accuracy of measurement, all electrical parameters of the filter for its three tuning channels were the same as under low RF input power (Table 1), provided appropriate diode bias was applied.

Figure 14 indicates the essentials of the high-power, CW, UHF test facility (much of which was Government furnished equipment). The RF source was an AN/ART-47 UHF transmitter operating in the CW mode and capable of being tuned in frequency steps of 50 kHz. (The transmitter frequency is set with precision by an internal frequency synthesizer and hence would never be subject to "pulling" by the load.) The transmitter could be followed optionally by an isolator/circulator which, although it diminished the RF power available for testing the filter, permitted the transmitter to operate with the frequency shifted to a 3-dB band-edge where the filter input VSWR is rather high (≈ 7).

Incident, transmitted, and reflected power for the filter were monitored by suitable directional and bidirectional couplers and Hewlett-Packard Type 8481A/435A power sensor/meter combinations, preceded by suitable "pads" to prevent overload of the sensors. As indicated in Figure 14, a short, lossless coaxial "through connection" could be inserted, in lieu of the test filter, between the transmitter and the final load, thereby permitting filter insertion loss to be evaluated directly and with precision by a substitution method. Additionally, the coefficients of the couplers and pads were known and used in measuring the absolute input and reflected power levels.

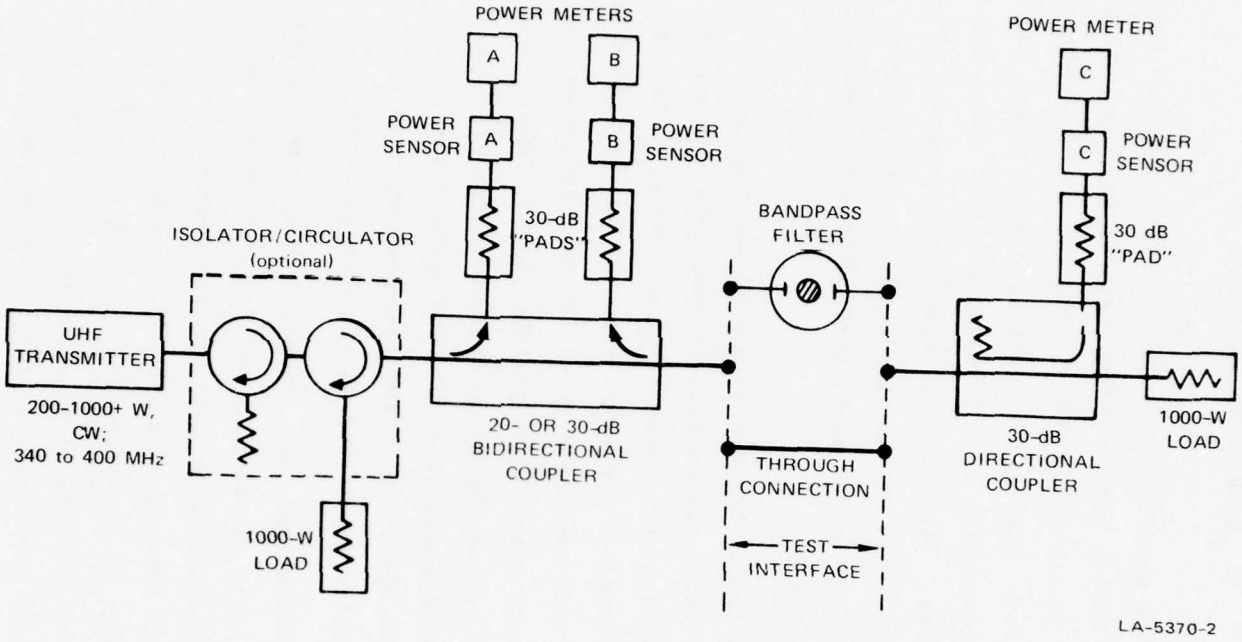

FIGURE 14 BLOCK DIAGRAM OF HIGH-POWER CW UHF TEST FACILITY

Figure 15 schematically indicates the feasibility-model bandpass filter connected to a suitable circuit for applying bias to the two sets of PIN diodes and selecting any one of the three possible channel-center frequencies. The microammeters that monitor diode leakage currents under reverse bias are important in the high-power tests. For low levels of RF input power, the leakage current does increase with bias voltage, but nevertheless remains low (≤ 4 μA at room temperature for 12 diodes at 650 V). At high levels of RF input power, the temperatures of the filter body and of the diodes rise, since as much as 13% of the RF input power plus the forward-bias power may be dissipated within the filter. When equilibrium is reached, the PIN chips are warmer than adjacent parts of the filter body by about 6°C per watt of dissipation within the chip (P_{dD}). Of itself, the diode temperature rise causes the leakage current to increase somewhat.* In addition, the RF drive voltage, $\hat{V}_1$, when large and superposed on the bias voltage, causes an increase in the leakage current reading because of the curvature of the reverse-current-versus-voltage curve for "soft-knee" diodes. In all, the reverse current can reach about 30 μA for 12 diodes at temperature equilibrium under 650 V of bias and 1250 W of RF input power. This current is quite modest and entirely "safe," since reverse currents of up to 10 μA per diode are easily tolerated.

It is also informative to observe the reverse leakage current, I_r, under fixed RF drive, $\hat{V}_1$, while slowly decreasing the bias voltage, V_0. Starting with $V_0 \geq V_1 + 250$ V, the decrease in V_0 initially causes I_r to decrease. However, when V_0 is in the vicinity of $\hat{V}_1$, I_r starts to increase, often rapidly. These effects are due to the fact that R_p (the effective shunt diode loss resistance) begins to decrease as $V_0 \rightarrow \hat{V}_1$.† The escalation in diode losses raises the diode temperature and

---

*This can be observed by operating at full rated power under forward bias until temperature equilibrium is reached, keying off the RF, and reading the leakage current under reverse bias immediately thereafter.

†The reasoning here is not qualitatively affected by the fact that the diodes in a pair are in a "push-pull" relationship. That is, at the instant when one is being driven toward a larger reverse voltage, the other is being driven the other way.

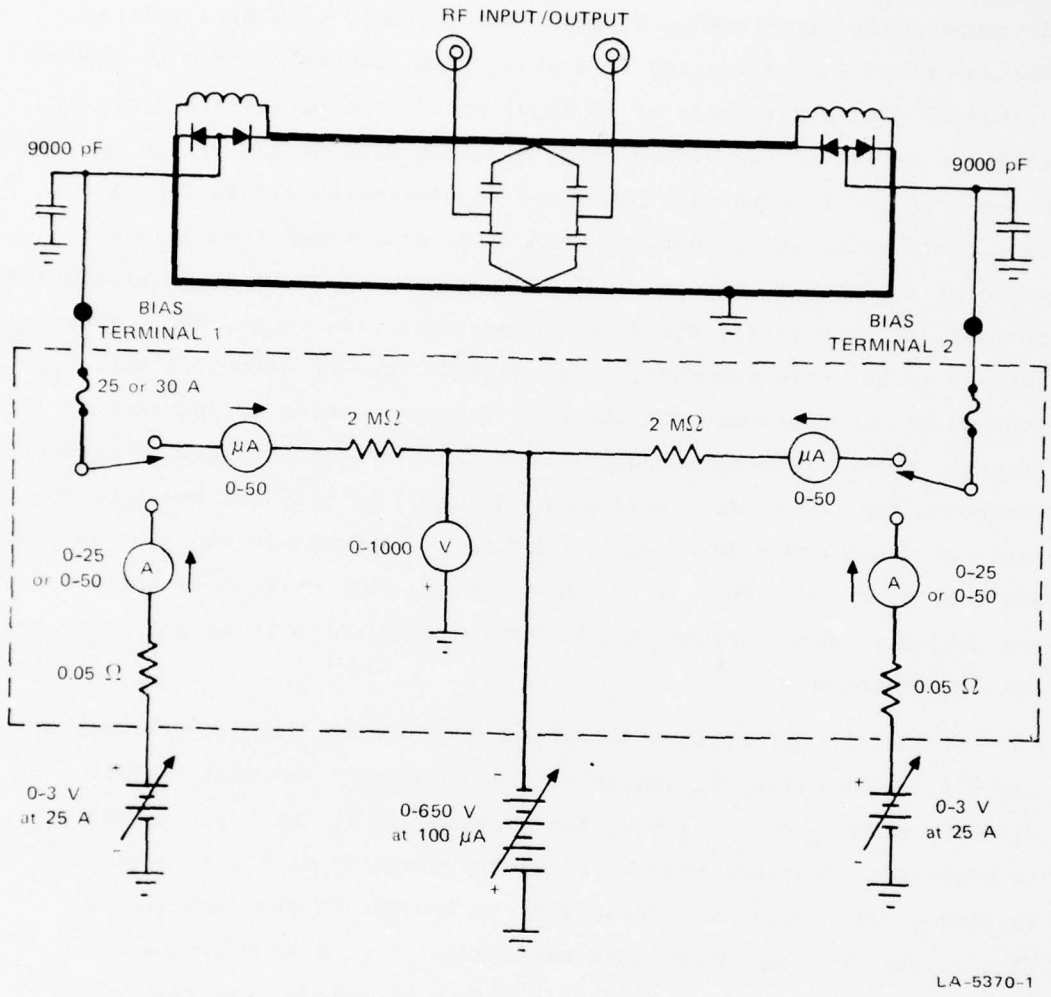

FIGURE 15 SCHEMATIC REPRESENTATION OF UHF BANDPASS FILTER AND DIODE BIASING MEANS

hence I_r. For CW operation at UHF, it appears that the diodes should be operated with $V_0 \geq \hat{V}_1 + 50$ V.* In confirmation of the foregoing, Figure 16 shows the variation of filter insertion loss with V_0 for fixed $\hat{V}_1 \approx 360$ V ($P_0 = 800$ W) at f_{0A}. Thus, while $V_0 \geq 250$ V is adequate under small signal conditions, $V_0 > 500$ V is recommended for full-power operation.†

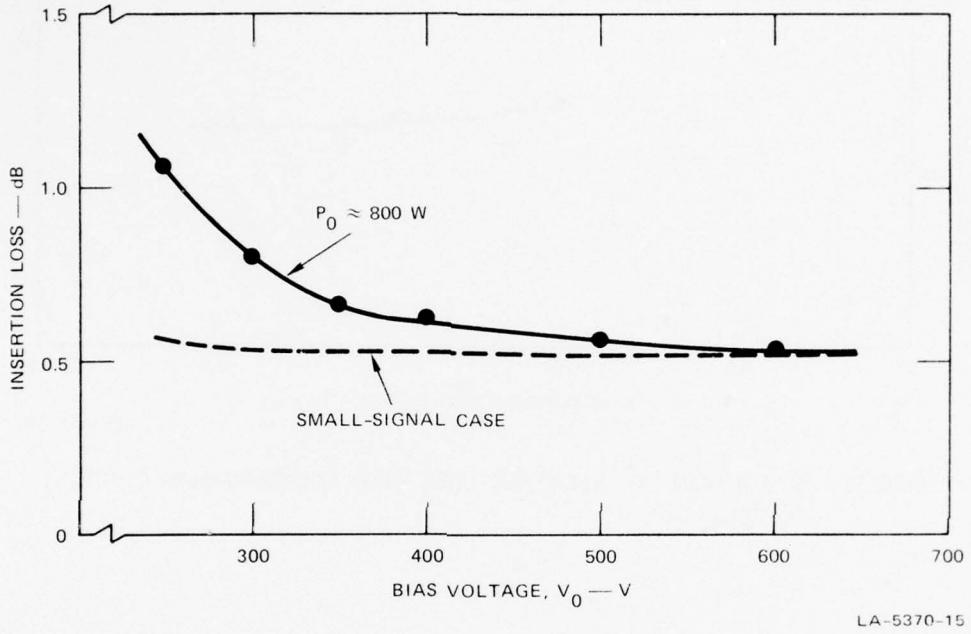

FIGURE 16 INSERTION LOSS vs REVERSE-BIAS VOLTAGE FOR HIGH-POWER OPERATION AT f_{0A}

---

*Because the frequency is sufficiently high, it is entirely possible to have $\hat{V}_1 \geq V_0$ without forward conduction, or even a change in diode capacitance, occurring. (With pulsed X-band and K-band signals, for example, the RF drive voltage can be quite large compared with the bias voltage.) However, when diode losses or intermodulation distortion are of concern, different recommendations may be necessary.

†With the filter operating at full rated RF input power at f_{0A}, the likelihood of RF leakage from the filter, via a "hot" bias feedthrough, is greatest. However, use of a Narda Model 8300 radiation monitor to search for such RF leakage gave negative results.

Under forward bias, the effective value of R_s is indifferent to RF level.* The variation of insertion loss with forward bias current under high input power (Figure 17) merely reflects the variation of Q_{uB} with bias current (Figure 13). It is interesting to observe that, below about 1.5 A for $P_0 \geq 1000$ W, an increment in bias current reduces the RF power dissipated by an amount that is greater than the bias power added.

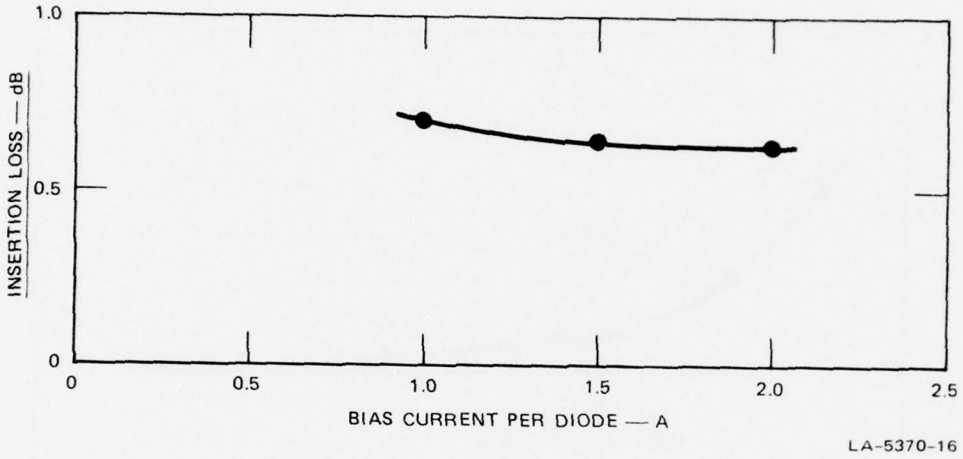

FIGURE 17 VARIATION OF INSERTION LOSS WITH FORWARD-BIAS CURRENT AT f_{0B}

*This would be the case for RF currents up to roughly $f\tau$ ($\sim$ 2000) times the dc bias current, where τ ($\approx$ 5 μs) is the carrier lifetime for the PIN diode.

VII CONCLUSIONS

Establishing the feasibility of a low-loss, high-power UHF resonator having electronic tuning means based on PIN-diode control of series inductances (the "L-Flauto" concept) represents a significant advance over prior art. The usefulness of the approach is indicated by the achievement of unloaded Q values in the vicinity of 2000, and of a continuous internal volt-ampere rating of at least a few times 10^5 VA, for an overall tuning range of 11%. Improvements in Air Force communication systems should result if the new technology is used in producing either a fast-tuned transmitter-output-stage tank circuit or an ETF. Such an ETF could have a CW input power rating in excess of 1000 W, and a loaded bandwidth and insertion loss around 0.9% and 0.5 dB, respectively, per resonator.

The agreement between predicted and observed performance data attests to the aptness and validity of the equivalent-circuit modeling and of the design relations developed. Future work can thus be undertaken with confidence in the predicted outcome. The techniques introduced to facilitate and simplify resonator development and generate economies in the early phases of the program represent a significant contribution to the art. In particular, reference is made to the usefulness of dummy diodes and of a symmetrical model having two tuning elements, one of which is the first or most-significant of a binary-scaled series of tuning elements, and the other is a surrogate for all the remaining, less-significant tuning elements. The ease with which suitable PIN diodes can be selected, biased, and cooled was demonstrated, along with the advantages of grouping series pairs of them in parallel, with bias applied to the common-anode point of each pair and of the entire array.

It might be valuable to have a figure of merit by which to judge whether a resonator design is making the fullest use of its diodes, with

respect to RF input power rating. A general, dimensionless figure of merit might thus be written as

$$M \equiv \sqrt{2}\ P_0 Q_E \rho / (\hat{V}_1 \tilde{I}_{max} m)$$

where ρ is the fractional tuning range, m is the total number of diodes present, and $\tilde{I}_{max}$ is the rms diode current corresponding to the maximum allowable thermal stress. However, no design has been produced to date in which the diodes are thermally stressed to anywhere near their limit. Until such a design is developed, all the capabilities of the diodes will not be fully exploited.

In cases where the overall power rating is determined only by the diode voltage stress, a "stress admittance" defined as

$$Y_s \equiv 2P_0 \hat{V}_1^{-2}$$

makes a convenient figure of merit for comparing different designs having the same loaded bandwidth and overall tuning range. Thus, the C-type resonator developed under the previous contract is characterized by $Y_s \approx 0.36$ millimho, while the resonator developed under the current contract has $Y_s \approx 12.5$ millimhos, which is about 35 times greater.

The prediction and evaluation of intermodulation distortion (IMD) resulting from stressing the nonlinear capacitance of a reverse-biased diode at two different frequencies were not within the scope of the current contract. However, some pertinent remarks can be made. If the desired signal frequency, f_α, the spurious signal frequency, f_β, and the frequencies, $f_\gamma = 2f_\beta - f_\alpha$ and $f_\delta = 2f_\alpha - f_\beta$, of the third-order intermodulation products are all within $\frac{1}{2}\Delta f_3$ of f_{0A}, it is clear that the relation

$$P = \frac{1}{2} Y_s \hat{V}^2$$

is essentially valid in all four cases. (P is the power in the external cables associated with any of the four components, and $\hat{V}$ is the peak

voltage on a most-stressed diode due to this component.) Since IMD performance is expressed (by RADC) as the ratio of P_γ or P_δ to P_α (given the absolute magnitudes of P_α and P_β), the filter design is seen not to be a factor. That is, it should be sufficient to place a single diode of the type specified <u>in any circuit</u> where $\hat{V}_\alpha$ and $\hat{V}_\beta$ can be applied and $\hat{V}_\gamma$ and $\hat{V}_\delta$ measured, to express the eventual IMD performance of a filter as a power ratio.

Since the diodes in the new resonator are stressed about 53% as much as those in the previous resonator--under <u>rated</u> input power to the filter in both cases--one is tempted to predict a superior IMD performance for the new resonator. However, the previous resonator used series UM 7000 diodes rather than series UM 4000; hence, extrapolation based on previous work may not be reliable. Since it is known that IMD performance can be improved according to how large the bias voltage can be, relative to the RF voltages, the new resonator should be better in this regard.

VIII OPTIONS FOR FUTURE WORK

Three broad areas in which future work may be desirable are discussed below. The first consists of natural extensions of the current work toward realizing operational multichannel resonators, and toward size reduction via several possible approaches, all relying on the "lightly-loaded L-type" approach. The second area deals with "heavily-loaded C-type" resonators, which are considered as a possible alternative to realizing a low-loss, high-power resonator. The third area concerns application of all the concepts so far considered to needs that are more diverse than at present (as regards frequency band, for example).

It is understood that any resonator mentioned in this section would not only be usable (singly or multiply) in a bandpass filter, but might also serve as the fast-tuning "tank" circuit of a solid-state transmitter output stage. In the latter case the resonator would provide a "clean" spectrum, and it should also very conveniently serve the functions of combining and impedance matching for the necessary multiple active devices.

A. Extension of Current Work

It is assumed that the following performance objectives for an electronically tunable resonator will continue to apply:

- A tuning range of at least 12% within the UHF band (225 to 400 MHz, with preference for the high end)
- A product of loaded Q and RF power rating in the range of one to a few times 10^5 W
- An unloaded Q of at least 1000.

Hence, a natural extension of the work of the current contract is to apply its technology to the development of an operational multichannel resonator.

PRECEDING PAGE BLANK-NOT FILMED

Figure 18(a) illustrates the essential configuration of a 32-channel, single-resonator filter based directly on the design of Figures 9 and 10. That is, D_1, D_2, D_3, h, ℓ, n, R_s, R_p, and the cavity wall conductivity are preserved, but the duplicate of Tuning Element 1 is removed and replaced by Tuning Elements 2, 3, 4, ..., N, for which it was the surrogate. The performance of this filter would be predictable and satisfactory, but the overall volume could be unattractive.

Figure 18(b) represents the same design concept as Figure 18(a), except that all transverse dimensions have been halved, so that the overall volume is about 1/4 that applicable to Figure 18(a). No change in performance should result, except for an increase of the insertion loss by at most 0.4 dB. This resonator design offers the least uncertainty regarding the performance to be expected, along with an overall diameter of about 5 inches and length of about 14 inches for the tuning range 355 to 400 MHz. Of course, means for "trimming" the reactance of each tuning element, and for providing tuning increments smaller than 1/32 of the total tuning range, would need to be provided. The cooling needs of the less-significant tuning elements are relieved by the fact that the RF power dissipated in each tuning element is half that of the previous one. Some savings in diode costs can accrue from the fact that $\hat{V}_1$ for each tuning element is 0.707 times that of the previous one.

Figure 18(c) suggests a variation on the design of Figure 18(b) leading to a further reduction in overall volume. For tuning Element 1, h has been doubled so that D_3 can be substantially reduced (e.g., to 3 inches). This can be done because Tuning Element 1 stands fairly distant from any of the other tuning elements. In lieu of increasing h for Tuning Elements 2, 3, 4, ..., however, their distances from the resonator mid-plane have been increased so that the reduced value of D_3 may nevertheless provide the same tuning increments as before. In essence, the local value of X_1 for Tuning Elements 2, 3, 4, ..., N is about half that for Tuning Element 1. In this design, however, it can be shown that twice as many diode pairs as before must be parallelled in Tuning Element 2 (and beyond) in order that its power dissipation be half that of Tuning Element 1.

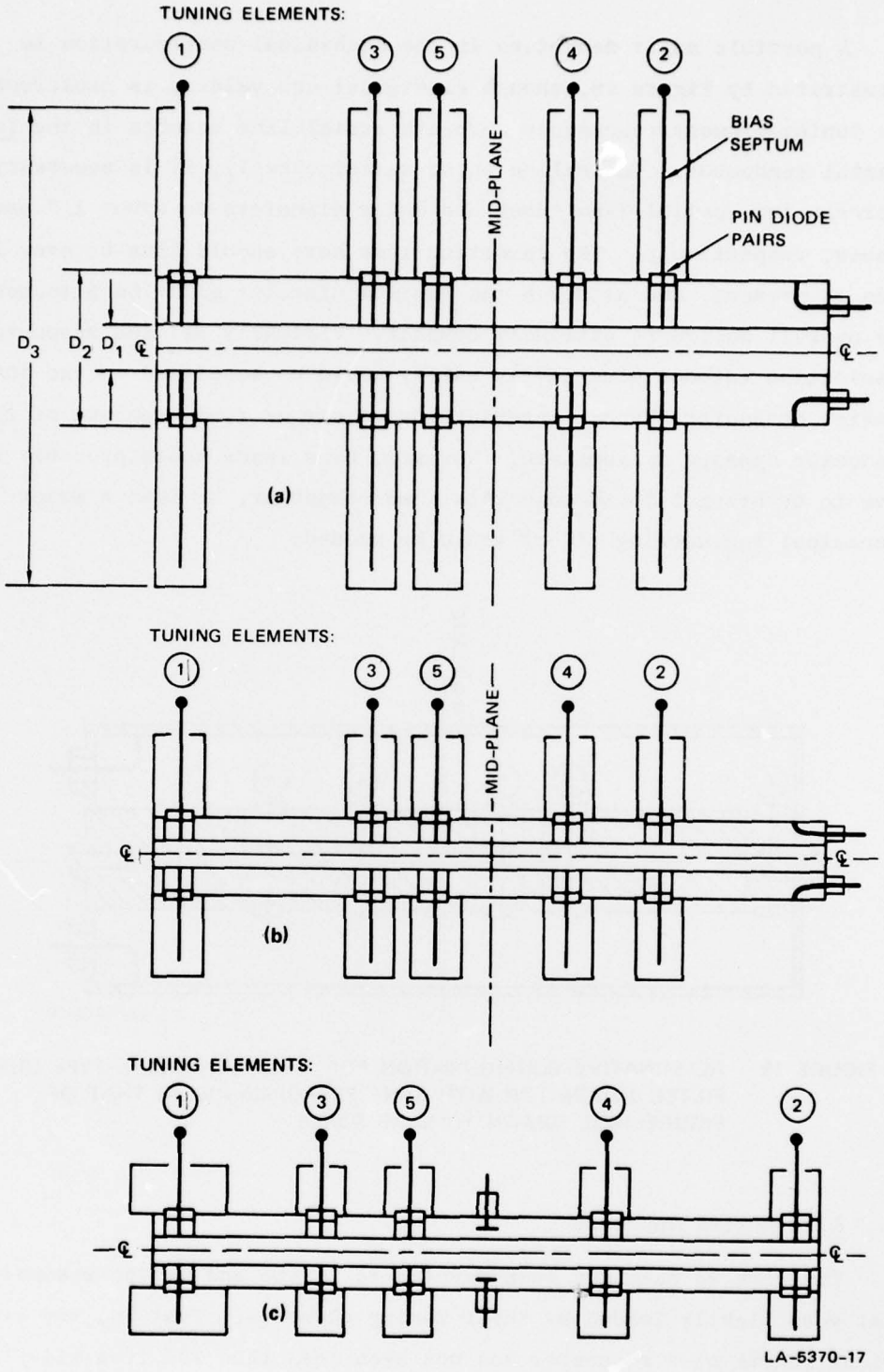

FIGURE 18 POSSIBLE CONFIGURATIONS FOR MULTICHANNEL L-TYPE HIGH-POWER UHF FILTER RESONATORS, DRAWN TO A SCALE OF ABOUT 1:3.3

A possible major departure in the mechanical configuration is illustrated by Figure 19, though electrical equivalence is preserved. The tuning-element reactances here are radial-line notches in the inner coaxial conductor. To realize these satisfactorily, it is necessary to increase the coaxial-line inner and outer diameters to about 1.7 and 5 inches, respectively. The insertion loss here should thus be even lower than at present, and although the maximum diameter might be 5 inches, the overall design is extremely compact. Virtually all the resonator dissipation (diodes plus cavity walls) would be localized in the inner coaxial conductor; hence, internal forced air or fluid cooling of this conductor appears appropriate. However, bias leads would probably also have to be brought in through this same conductor, so that a major mechanical engineering effort would be needed.

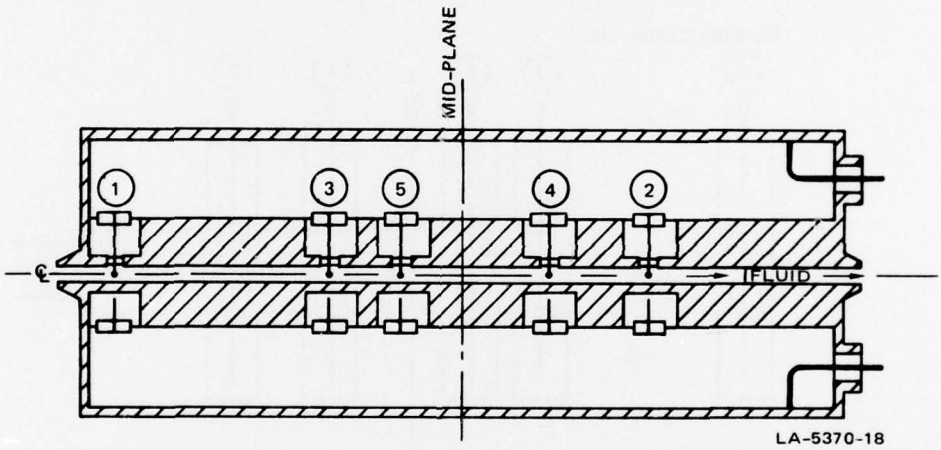

FIGURE 19 ALTERNATIVE CONFIGURATION FOR MULTICHANNEL L-TYPE UHF FILTER RESONATOR WITH SAME PERFORMANCE AS THAT OF FIGURE 18(a), DRAWN TO SAME SCALE

B. Alternative Approach

The work to date has been devoted to L-type and C-type resonators that were lightly loaded by their tuning elements. That is, the electrical length of a resonator has not been less than 70° from mid-plane to a short-circuited end. However, some interesting predictions result

when one models a heavily-loaded C-type resonator--i.e., one in which the total effective tuning capacitance is so large that the resonator electrical length would be less than 30° and hence effectively constitute a lumped inductance. An analysis indicates that substantial increases in Y_s relative to that for lightly-loaded C-type resonators should result.* For example, a value of $Y_s \approx 6$ millimhos appears feasible, permitting $P_0 \approx 1000$ W with "1000-volt" diodes.

This approach, considered for UHF and lower frequencies, inherently leads to rather compact designs. It also leads to the abandonment of spatially distributed, equal tuning elements in favor of localized, unequal tuning capacitances. In this case certain advantages accrue, but some problems are also apparent. Further investigations would be necessary to establish the usefulness of the nondistributed, heavily-loaded, C-type approach to electronic resonator tuning.

C. Other Areas of Application

The techniques investigated under the current and previous contracts should be adaptable to many applications wherever low-loss (high Q_u), narrow-bandwidth (high Q_L) resonators require electronic tuning based on PIN diodes to avoid the signal-level limitations imposed by devices such as varactors. Although the specifications might be diverse as regards frequency band, power rating, duty cycle, instantaneous bandwidth, etc., it would be worthwhile to consider the technology developed under SRI's three contracts in responding to the application need.

---

*This was first pointed out by W.A. Edson.

Appendix A

EFFECTS OF FINITE DIODE REACTANCE ON DESIGN RELATIONS

PRECEDING PAGE BLANK-NOT FILMED

Appendix A

EFFECTS OF FINITE DIODE REACTANCE ON DESIGN RELATIONS

1. Reverse-Bias Case

In Section III-D, the reverse-biased-diode capacitance, C_D, was assumed to be zero. With C_D nonzero, the net inductive reactance of the tuning element is

$$X_1 = \frac{X_{SA} X_C}{X_C - X_{SA}}$$

where

$$X_C = [2\pi f_{0A} n C_D/2]^{-1}$$

and X_{SA} is the input reactance of the radial line at frequency f_{0A}.* For $C_D \approx 3$ pF, maximum, and $f_{0A} \approx 355$ MHz, X_C would not be less than about (300/n) ohms, yielding 50 ohms for n = 6 (or 37.5 ohms for n = 8). To obtain $X_1 = 11$ ohms with $C_D > 0$, so as to leave the tuning range and the RF voltages unaffected, one might design the radial line to give X_{SA} = 9 ohms (or 8.5 ohms if n = 8 instead of 6).

In essence, the diode capacitance provides a positive trimming effect for the effective inductance of the radial line. In fact, in future work it might actually be convenient to trim a tuning reactance by means of adjustable high-voltage capacitors installed in parallel with the diodes. A necessary precaution would be to ensure that the resonance of X_S with the total X_C would occur well above the tuning range.

---

*It is being assumed that $X_C \gg$ the inductive reactance $2\pi f_{0A}(2L_D/n)$ with which it is in series (Figure 6).

PRECEDING PAGE BLANK-NOT FILMED

2. Forward-Bias Case

At f_{0B}, a nonzero switch inductance of $2L_D/n$, rather than a short circuit, appears across the input reactance of the radial line, X_{SB}. (To a first approximation, $X_{SB} \approx X_{SA} f_{0B}/f_{0A}$.) The net inductive reactance, X_{min}, provided by X_{SB} in parallel with $X_{DB} \equiv 2\pi f_{0B}(2L_D/n)$, will be only slightly smaller than X_{DB}, since $X_{SB} >> X_{DB}$.

The major consequence of having $X_{min} > 0$ is that the resonator half-length, ℓ, would need to be shortened slightly to ℓ' to maintain a specified f_{0B}. The relation

$$\frac{X_{min}}{Z_0} = \cot\left(\frac{\pi}{2}\frac{\ell'}{\ell}\right)$$

expresses the necessary correction. Having shortened ℓ to ℓ', a small increase in X_1 to X_1' would then be necessary to maintain a specified f_{0A}. The relation

$$\frac{X_1'}{Z_0} = \cot\left(\frac{\pi}{2}\frac{f_{0A}}{f_{0B}}\frac{\ell'}{\ell}\right)$$

expresses the necessary correction. With X_1 increased to X_1', the RF voltage stress on a reverse-biased diode will be correspondingly larger.

For example, with $Z_0 = 63$ ohms and a resonator half-length of 7.25 inches, the resonant frequency observed (Section V-A-2) with all diodes forward-biased (and under minimal coupling-probe penetration) was 401.6 MHz instead of the 407.3 MHz that corresponds to $\lambda = 4 \times 7.25$ inches. This result is consistent with $\ell'/\ell = 0.985$, from which it appears that the value of X_{min} resulting from the actual array of six diode pairs and their contact springs is about 1.35 ohms, or 2% of Z_0. Correspondingly, X_1' should be made about 11% larger than would be required for $X_{min} \rightarrow 0$, and the RF voltage stress at f_{0A} would then be about 11% greater than estimated. With the mounting and contact spring arrangement chosen, the effective inductance of each diode is thus

estimated to be about 1.8 nanohenries. (The relevant manufacturer's literature states merely that the glassed portion of the diode alone has an inductance "on the order of 0.1 nanohenry.")

Appendix B

DERIVATION OF EXPRESSIONS FOR UNLOADED Q

PRECEDING PAGE BLANK-NOT FILMED

Appendix B

DERIVATION OF EXPRESSIONS FOR UNLOADED Q

1. Forward-Bias Case

Figure B-1 is the applicable equivalent circuit. The series-resonant elements L_ℓ and C_ℓ represent a symmetrical half of the filter resonator, as seen at a shorted end, looking toward the mid-plane. From "slope parameter" theory, one can write

$$2\pi f_{0B} L_\ell = \frac{\pi}{4} Z_0$$

which is exact at f_{0B}. The resistance $R_{\ell B}$ represents all resonator losses except those due to the diodes; thus,

$$Q_{u\ell B} = \frac{2\pi f_{0B} L_\ell}{R_{\ell B}} = \frac{\pi Z_0}{4R_{\ell B}} \quad .$$

If diode inductance is neglected, the diode array provides an additional resistance, $2R_s/n$, at the shorted end of the resonator.

The overall Q_u is thus

$$Q_{uB} = \frac{2\pi f_{0B} L_\ell}{R_{\ell B} + 2R_s/n} = \frac{Q_{u\ell B} Q_{u1B}}{Q_{u\ell B} + Q_{u1B}}$$

or

$$\frac{1}{Q_{uB}} = \frac{1}{Q_{u\ell B}} + \frac{1}{Q_{u1B}}$$

where

$$Q_{u1B} \equiv n\pi Z_0/8R_s \quad .$$

PRECEDING PAGE BLANK-NOT FILMED

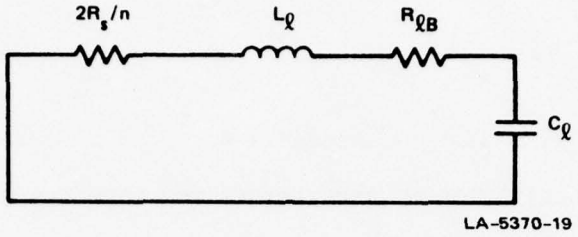

FIGURE B-1 EQUIVALENT CIRCUIT, USING SLOPE-PARAMETER VALUES, FOR RESONATOR WITH FORWARD-BIASED DIODES AT FREQUENCY f_{0B}

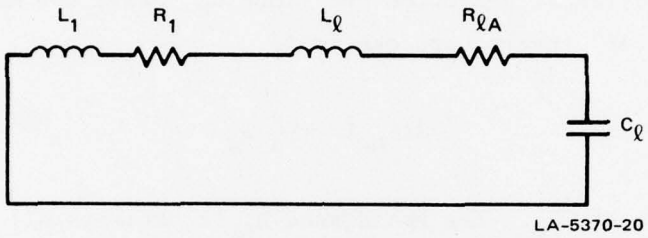

FIGURE B-2 EQUIVALENT CIRCUIT, USING SLOPE-PARAMETER VALUES, FOR RESONATOR WITH REVERSE-BIASED DIODES AT FREQUENCY f_{0A}

2. Reverse-Bias Case

Figure B-2 is the equivalent circuit applicable at f_{0A}. If diode capacitance is neglected, the tuning element is represented by L_1 and R_1, such that

$$2\pi f_{0A} L_1 \equiv X_1$$

and

$$R_1 \equiv nX_1^2/2R_p \quad .$$

(That is, the series combination of L_1 and R_1 is closely equivalent to the shunt combination of L_1 and $2R_p/n$.) Moreover, a tuning-element Q can be defined by

$$Q_{XA} \equiv 2R_p/nX_1 \quad .$$

As before, the coaxial half-resonator, viewed from the tuning element toward the mid-plane, is represented by the slope-parameter elements L_ℓ and C_ℓ, in series. The expression

$$2\pi f_{0B} L_\ell = \frac{\pi}{4} Z_0$$

applies, but the implied effective value of L_ℓ will be less exact when the frequency drops from f_{0B} to f_{0A}. The cavity-loss equivalent resistance, $R_{\ell A}$, satisfies

$$Q_{u\ell A} = \frac{2\pi f_{0A}(L_\ell + L_1)}{R_{\ell A}}$$

and, since $Q_{u\ell A}$ would be determined experimentally, $R_{\ell A}$ can include the effects of any losses associated with the tuning element other than those occurring in the diodes.

The overall Q_u, therefore, is

$$Q_{uA} = \frac{2\pi f_{0A}(L_\ell + L_1)}{R_{\ell A} + R_1}$$

which, after algebraic manipulation, becomes

$$Q_{uA} = \frac{KQ_{XA}Q_{u\ell A}}{KQ_{XA} + Q_{u\ell A}}$$

or

$$\frac{1}{Q_{uA}} = \frac{1}{KQ_{XA}} + \frac{1}{Q_{u\ell A}}$$

where

$$K \equiv 1 + \frac{\pi}{4} \frac{f_{OA}}{f_{OB}} \frac{Z_O}{X_1} \quad .$$

Thus, although Q_{XA} may itself be modest in value, its contribution to the overall Q_{uA} is effectively magnified by the factor K.

REFERENCES

1. A. Karp and W. B. Weir, "Electronically Tunable High-Power Filter for Interference Reduction in Air Force Communications Systems," Final Report, Contract F30602-71-C-0255, SRI Project 1201, Stanford Research Institute, Menlo Park, Calif. (June 1972), RADC-TR-72-196, (748810).
2. A. Karp and L. N. Heynick, "UHF Electronically Tunable High Power Filter," Final Report, Contract F30602-74-C-0142, SRI Project 3321, Stanford Research Institute, Menlo Park, Calif. (September 1975), RADC-TR-75-220, (A018044).
3. S. Ramo and J. R. Whinnery, Fields and Waves in Modern Radio, 1st Ed., pp. 354-360 (John Wiley and Sons, Inc., New York, N.Y., 1944).
4. G. L. Matthaei, L. Young, and E. M. T. Jones, Microwave Filters, Impedance-Matching Networks, and Coupling Structures, p. 920 (McGraw-Hill Book Company, New York, N.Y., 1964).
5. G. K. Farney, "An Electronically Tuned, Pulsed Coaxial Magnetron for K_u Band," Final Report, Contract N00123-75-C-0911, Varian Associates, Beverly, Mass. (16 August 1976).
6. "Microwave Network Analyzer Applications," Application Note 117-1, pp. 8-7 to 8-9, Hewlett-Packard Co., Palo Alto, Calif. (June 1970).

METRIC SYSTEM

BASE UNITS:

Quantity	Unit	SI Symbol	Formula
length	metre	m	...
mass	kilogram	kg	...
time	second	s	...
electric current	ampere	A	...
thermodynamic temperature	kelvin	K	...
amount of substance	mole	mol	...
luminous intensity	candela	cd	...

SUPPLEMENTARY UNITS:

plane angle	radian	rad	...
solid angle	steradian	sr	...

DERIVED UNITS:

Acceleration	metre per second squared	...	m/s
activity (of a radioactive source)	disintegration per second	...	(disintegration)/s
angular acceleration	radian per second squared	...	rad/s
angular velocity	radian per second	...	rad/s
area	square metre	...	m
density	kilogram per cubic metre	...	kg/m
electric capacitance	farad	F	A·s/V
electrical conductance	siemens	S	A/V
electric field strength	volt per metre	...	V/m
electric inductance	henry	H	V·s/A
electric potential difference	volt	V	W/A
electric resistance	ohm		V/A
electromotive force	volt	V	W/A
energy	joule	J	N·m
entropy	joule per kelvin	...	J/K
force	newton	N	kg·m/s
frequency	hertz	Hz	(cycle)/s
illuminance	lux	lx	lm/m
luminance	candela per square metre	...	cd/m
luminous flux	lumen	lm	cd·sr
magnetic field strength	ampere per metre	...	A/m
magnetic flux	weber	Wb	V·s
magnetic flux density	tesla	T	Wb/m
magnetomotive force	ampere	A	...
power	watt	W	J/s
pressure	pascal	Pa	N/m
quantity of electricity	coulomb	C	A·s
quantity of heat	joule	J	N·m
radiant intensity	watt per steradian	...	W/sr
specific heat	joule per kilogram-kelvin	...	J/kg·K
stress	pascal	Pa	N/m
thermal conductivity	watt per metre-kelvin	...	W/m·K
velocity	metre per second	...	m/s
viscosity, dynamic	pascal-second	...	Pa·s
viscosity, kinematic	square metre per second	...	m/s
voltage	volt	V	W/A
volume	cubic metre	...	m
wavenumber	reciprocal metre	...	(wave)/m
work	joule	J	N·m

SI PREFIXES:

Multiplication Factors	Prefix	SI Symbol
1 000 000 000 000 = 10^{12}	tera	T
1 000 000 000 = 10^{9}	giga	G
1 000 000 = 10^{6}	mega	M
1 000 = 10^{3}	kilo	k
100 = 10^{2}	hecto*	h
10 = 10^{1}	deka*	da
0.1 = 10^{-1}	deci*	d
0.01 = 10^{-2}	centi*	c
0.001 = 10^{-3}	milli	m
0.000 001 = 10^{-6}	micro	μ
0.000 000 001 = 10^{-9}	nano	n
0.000 000 000 001 = 10^{-12}	pico	p
0.000 000 000 000 001 = 10^{-15}	femto	f
0.000 000 000 000 000 001 = 10^{-18}	atto	a

* To be avoided where possible.

MISSION
of
Rome Air Development Center

RADC plans and conducts research, exploratory and advanced development programs in command, control, and communications (C^3) activities, and in the C^3 areas of information sciences and intelligence. The principal technical mission areas are communications, electromagnetic guidance and control, surveillance of ground and aerospace objects, intelligence data collection and handling, information system technology, ionospheric propagation, solid state sciences, microwave physics and electronic reliability, maintainability and compatibility.